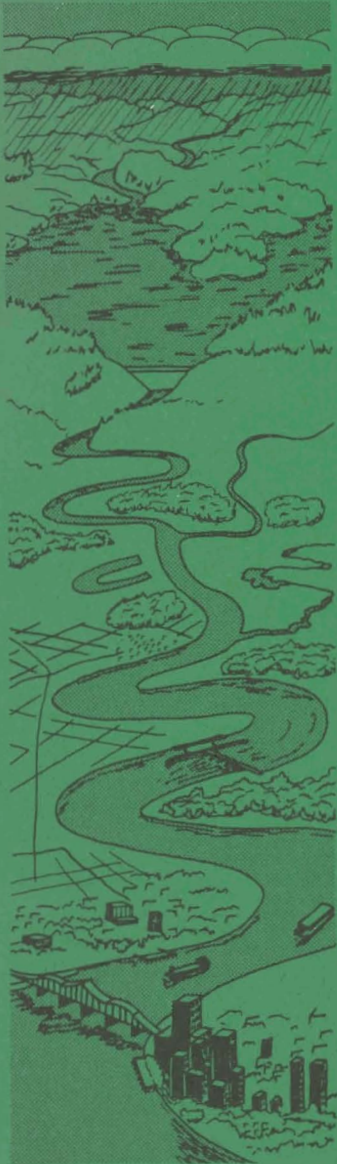




US Army Corps  
of Engineers



# HYDRAULICS LAB COPY

ENVIRONMENTAL AND WATER QUALITY  
OPERATIONAL STUDIES

TECHNICAL REPORT E-87-6

## HYDRODYNAMICS AND MODELING OF REREGULATION POOLS

by

R. C. Berger, Jr.

Hydraulics Laboratory

DEPARTMENT OF THE ARMY  
Waterways Experiment Station, Corps of Engineers  
PO Box 631, Vicksburg, Mississippi 39180-0631



May 1987

Final Report

Approved For Public Release; Distribution Unlimited

Prepared for DEPARTMENT OF THE ARMY  
US Army Corps of Engineers  
Washington, DC 20314-1000

Under EWQOS Task IIIB

Monitored by Environmental Laboratory  
US Army Engineer Waterways Experiment Station  
PO Box 631, Vicksburg, Mississippi 39180-0631



**REPORT DOCUMENTATION PAGE**

1a. REPORT SECURITY CLASSIFICATION Unclassified		1b. RESTRICTIVE MARKINGS	
2a. SECURITY CLASSIFICATION AUTHORITY		3. DISTRIBUTION / AVAILABILITY OF REPORT Approved for public release; distribution unlimited	
2b. DECLASSIFICATION / DOWNGRADING SCHEDULE		5. MONITORING ORGANIZATION REPORT NUMBER(S)	
4. PERFORMING ORGANIZATION REPORT NUMBER(S) Technical Report E-87-6		7a. NAME OF MONITORING ORGANIZATION USAEWES Environmental Laboratory	
6a. NAME OF PERFORMING ORGANIZATION USAEWES Hydraulics Laboratory	6b. OFFICE SYMBOL (if applicable) WES HL	7b. ADDRESS (City, State, and ZIP Code) PO Box 631 Vicksburg, MS 39180-0631	
6c. ADDRESS (City, State, and ZIP Code) PO Box 631 Vicksburg, MS 39180-0631		9. PROCUREMENT INSTRUMENT IDENTIFICATION NUMBER	
8a. NAME OF FUNDING / SPONSORING ORGANIZATION See reverse	8b. OFFICE SYMBOL (if applicable) DAEN	10. SOURCE OF FUNDING NUMBERS	
8c. ADDRESS (City, State, and ZIP Code) Washington, DC 20314-1000		PROGRAM ELEMENT NO.	PROJECT NO.
11. TITLE (Include Security Classification) Hydrodynamics and Modeling of Reregulation Pools		TASK NO.	WORK UNIT ACCESSION NO.
12. PERSONAL AUTHOR(S) Berger, R. C., Jr.			
13a. TYPE OF REPORT Final report	13b. TIME COVERED FROM Oct 82 TO Sep 84	14. DATE OF REPORT (Year, Month, Day) May 1987	15. PAGE COUNT 88
16. SUPPLEMENTARY NOTATION Available from National Technical Information Service, 5285 Port Royal Road, Springfield, VA 22161.			
17. COSATI CODES		18. SUBJECT TERMS (Continue on reverse if necessary and identify by block number)	
FIELD	GROUP	Hydraulic models (LC)	
		Hydrodynamics (LC)	
		Reservoirs (LC)	
19. ABSTRACT (Continue on reverse if necessary and identify by block number) A reregulation dam is used to reduce drastic flow fluctuations from main reservoir releases, usually as a consequence of hydropower operations. In a pumped-storage system, it also provides storage for subsequent pumpback to the upstream reservoir. This report describes the expected impact of the addition of a reregulation facility on the temperature regimen of the reservoir-reregulation pool system. A cost-effective method for simulating the hydrodynamics and transport in a reregulation pool is presented. The method has been coupled with a vertical one-dimensional reservoir model to simulate the hydrodynamics and transport of the reservoir-reregulation pool system.  The modeling procedure for simulating the hydrodynamics and transport of the reregulation pool was selected from three candidate methods. The three methods in progressive order of complexity are: (1) the sump method, (2) the level pool routing method, and (3) the finite difference simulation of the Saint-Venant equations. The methods have been (Continued)			
20. DISTRIBUTION / AVAILABILITY OF ABSTRACT <input checked="" type="checkbox"/> UNCLASSIFIED / UNLIMITED <input type="checkbox"/> SAME AS RPT. <input type="checkbox"/> DTIC USERS		21. ABSTRACT SECURITY CLASSIFICATION Unclassified	
22a. NAME OF RESPONSIBLE INDIVIDUAL		22b. TELEPHONE (Include Area Code)	22c. OFFICE SYMBOL

Unclassified

SECURITY CLASSIFICATION OF THIS PAGE

8a. NAME OF FUNDING/SPONSORING ORGANIZATION (Continued).

Environmental Water Quality Operational Studies  
US Army Corps of Engineers

19. ABSTRACT (Continued).

incorporated within the WESTEX model, and the predicted temperature profiles in the main reservoir and the release temperatures from the reregulation pool are compared to results from a reservoir study previously conducted at the Waterways Experiment Station. The longitudinal resolution of the level pool routing and the Saint-Venant simulation methods allow a more realistic response to temperature fluctuations than can be provided by the sump method. Further, the level pool routing method gives results comparable to the more complex Saint-Venant method in a more cost-effective manner.

Unclassified

SECURITY CLASSIFICATION OF THIS PAGE

## PREFACE

This study was conducted by the Hydraulics Laboratory (HL) of the US Army Engineer Waterways Experiment Station (WES), Vicksburg, Miss., during the period October 1982 through September 1984. The work was conducted under the Environmental and Water Quality Operational Studies (EWQOS) Work Unit No. IA.9, "Hydrodynamics of Reregulation Pools." The EWQOS was sponsored by the Office, Chief of Engineers, US Army, and was monitored by the Environmental Laboratory (EL) of WES.

The study was initiated by Mr. Jeffery P. Holland and completed by Mr. R. C. Berger, Jr., of the Reservoir Water Quality Branch (RWQB), Hydraulic Structures Division (HSD), WES, HL. Mr. Berger prepared this report and it was subsequently reviewed by Messrs. F. A. Herrmann, Jr., Chief of HL; John L. Grace, Jr., Chief, HSD, HL; and Holland, Chief, RWQB. Dr. Jerome H. Mahloch managed the project for the EWQOS under the general supervision of Dr. John Harrison, Chief, EL. This report was edited by Ms. Gilda Shurden, and text and figure layout was coordinated by Mrs. Chris Habeeb, Information Products Division, Information Technology Laboratory, WES.

COL Allen F. Grum, USA, was the previous Director of WES.  
COL Dwayne G. Lee, CE, is the present Commander and Director.  
Dr. Robert W. Whalin is Technical Director.

## CONTENTS

	<u>Page</u>
PREFACE.....	1
CONVERSION FACTORS, NON-SI TO SI (METRIC) UNITS OF MEASUREMENT.....	3
PART I: INTRODUCTION.....	4
Background.....	4
Objective.....	5
Scope.....	5
PART II: REVIEW OF LITERATURE.....	7
Reservoir Dynamics.....	7
Numerical Description of the Reservoir.....	10
Numerical Flow Description for the Reregulation Pool.....	13
PART III: METHODS OF ANALYSIS.....	17
Analytic Analysis.....	17
Numerical Modeling Analysis.....	32
PART IV: NUMERICAL COMPARISON OF METHODS.....	46
Description of Tests.....	46
Results.....	48
Discussion.....	54
PART V: SUMMARY AND CONCLUSIONS.....	57
Summary.....	57
Conclusions.....	57
REFERENCES.....	60
TABLES 1 and 2	
APPENDIX A: SAINT-VENANT EQUATIONS.....	A1
APPENDIX B: HYDRODYNAMIC CODE.....	B1
APPENDIX C: TRANSPORT CODE.....	C1
APPENDIX D: NOTATION.....	D1

CONVERSION FACTORS, NON-SI TO SI (METRIC)  
UNITS OF MEASUREMENT

Non-SI units of measurement in this report can be converted to SI (metric) units as follows:

<u>Multiply</u>	<u>By</u>	<u>To Obtain</u>
acres	4046.873	square metres
acre-feet	1233.489	cubic metres
BTU (International Table)	1055.056	joules
cubic feet	0.02831685	cubic metres
cubic feet per second	0.02831685	cubic metres per second
Fahrenheit degrees	5/9	Celsius degrees or Kelvins*
feet	0.3048	metres
feet per mile	0.1893935	metres per kilometre
feet <sup>2</sup> per second	9.290304	square metres per second
miles (US statute)	1.609347	kilometres
pounds (mass) per cubic foot	16.01846	kilograms per cubic metres
square feet	0.09290304	square metres

---

\* To obtain Celsius (C) temperature readings from Fahrenheit (F) readings, use the following formula:  $C = (5/9)(F - 32)$ . To obtain Kelvin (K) readings, use:  $K = (5/9)(F - 32) + 273.15$ .

# HYDRODYNAMICS AND MODELING OF REREGULATION POOLS

## PART I: INTRODUCTION

### Background

1. Gaining the full potential of our water resources can often cause conflicts between the various uses. In the case of a hydropower or water-supply reservoir, the demands for each use may be at the expense of conditions downstream. For example, consider Figure 1 in which hydropower operations designed for peaking power production generally induce marked pulsations in flow during the day; further,

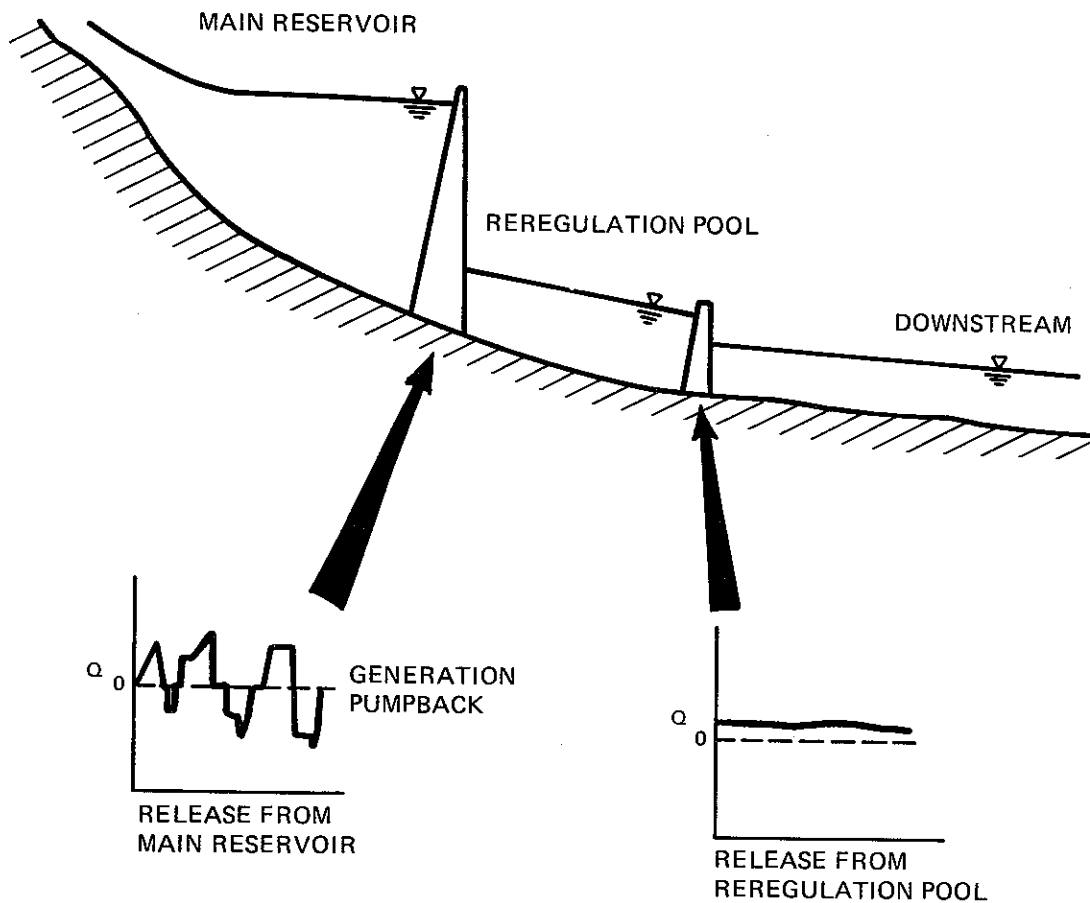


Figure 1. Layout of reservoir-reregulation pool system and the smoothing of hydropower operations

weekend shutdowns may drastically curtail flow in the downstream area causing wide fluctuations in downstream water quality (particularly temperature). This wide flow variation can result in environmental shock from the rapid change in temperature and dissolved oxygen. Auxiliary hydraulic structures, referred to as reregulation structures (Figure 1), are often employed just downstream of hydropower facilities to impound the highly variable releases from these projects. Thus, the presence of the reregulation pool will alleviate these downstream problems to some degree.

2. In addition to the reregulation of flow, some reregulation pools are used as a part of a pumped-storage system. In this system, the reregulation pool stores water from generation activities during peak demand periods so that some portion of it can be pumped back into the upstream reservoir during off-peak hours. In this manner, the water quality of each reservoir becomes dependent upon the other.

3. The design of a reregulation pool should therefore consider more than just the proper storage to provide a uniform discharge. The effect of the pool upon both upstream (for pumped storage) and downstream water quality should be analyzed. Otherwise, there may be cause for operational revisions which could impair the efficient use of the reservoir system.

#### Objective

4. The purpose of this study was to provide insight into the potential temperature impact of a reregulation facility and to develop an effective hydrodynamic model to provide input in the simulation of the transport of temperature and conservative constituents in a reservoir-reregulation pool system.

#### Scope

5. The potential impact of a reregulation pool on water-quality constituents will be demonstrated through the use of previous

investigations and simplified analytical models. These analytical models will also demonstrate the limitations of the candidate modeling techniques used to simulate the reregulation pool. The modeling of transport in a reregulation pool hinges upon adequate simulation of the hydrodynamics. The most effective means of simulating the hydrodynamics in a reregulation pool will be evaluated by comparing the results of progressively sophisticated modeling procedures.

## PART II: REVIEW OF LITERATURE

### Reservoir Dynamics

6. The proper simulation of the reregulation pool and its interaction with the surrounding systems requires an understanding of the major physical phenomena affecting the reservoir-reregulation pool system. Such understanding will allow the important features to be simulated at the resolution necessary. Thermal stratification is a major reservoir feature; it has a profound influence upon the reservoir's circulation and the resulting water quality distribution. Density stratification is a result of the effect of temperature on water density, the low thermal conductivity of water, the limited penetration of heat through the air-water interface, and the seasonal variation of stream temperatures and meteorological conditions. The mechanics of stratification have been described by Hutchinson (1957) and Kittrell (1965). They conclude that at the beginning of spring the reservoir has a virtually uniform vertical density profile. During spring the rate at which heat is distributed downward is soon exceeded by the rate of incoming heat. Most of the energy is absorbed near the surface. Since warm water is less dense it floats over the cool water and a definite temperature gradient develops, thus this gradient increases during the summer months of high energy input. The diurnal climatic temperature fluctuations and wind cause mixing of the surface layers forming a surface region of relatively uniform temperature called the epilimnion. The deeper regions of the pool remain cool due to the stable density stratification which has developed. This lower region of near uniform density is called the hypolimnion. The transition region is termed the metalimnion. Within the metalimnion, the elevation which has the greatest vertical temperature gradient is called the thermocline. In the fall, the epilimnion grows as a result of surface cooling which causes the denser surface water to sink. This causes mixing which eventually results in isothermal conditions again by the beginning of spring.

7. Determination of whether or not a reservoir will be stratified for particular conditions is somewhat difficult. However, there are a few methods that give some general indications.

8. Jirka and Watanabe (1980) developed a nondimensional number characterizing the ratio of destratifying and stratifying forces in a cooling pond. This number is referred to as the pond number  $P^*$  and is defined by

$$P = \left( \frac{f_i}{4} \frac{Q_o^2}{\beta \Delta T_o g H^3 W^2} D_v^3 \frac{L}{H} \right)^{1/4} \quad (1)$$

where

- $f_i$  = interfacial friction factor
- $Q_o$  = condenser flow rate
- $\beta$  = coefficient of thermal expansion for water
- $\Delta T_o$  = total temperature difference ( $T_o - T_i$ ) across pond
- $T_o$  = discharge temperature (into pond)
- $T_i$  = intake temperature (from pond)
- $g$  = gravitational acceleration constant
- $H$  = average pond depth
- $W$  = average pond width
- $D_v$  = vertical entrance dilution
- $L$  = total pond length

Jirka and Harleman (1979) have found that cooling ponds obey a one-dimensional temperature structure (only longitudinal variation exists) when  $L/W \geq 4$  and  $P \geq 1.0$ . Ponds for which  $L/W \geq 4$  and  $0.3 \leq P \leq 1.0$  may be analyzed as one dimensional (longitudinal) if allowance is made for thermal stratification in evaluating the surface-heat flux. Ponds in which  $P < 0.3$  were found to be vertically well stratified.

---

\* For convenience, symbols and abbreviations are listed in the Notation (Appendix D).

9. Orlob (1969) suggested the use of the densimetric Froude number to assess the potential for vertical stratification in a lake. The number is evaluated as:

$$F_D = \frac{LQ}{HV} \left( \frac{1}{ge} \right)^{1/2} \quad (2)$$

where

$F_D$  = densimetric Froude number

$L$  = length of the reservoir in ft

$Q$  = flow-through rate in cfs

$H$  = mean reservoir depth in ft

$V$  = volume of the reservoir in ft<sup>3</sup>

$g$  = gravitational acceleration 32.2 ft/sec<sup>2</sup>\*

$e$  = average normalized density gradient taken as  $0.3 \times 10^{-6}$ /ft

The value of the densimetric Froude number that marks the transition between the dominance of inertial forces and the dominance of gravitational forces Orlob takes to be  $1/\pi$ . For values below  $1/\pi$ , a strong vertical stratification pattern will exist.

10. Huber and Harleman (1968) listed the ratio  $R$  of yearly reservoir inflow volume to actual reservoir volume for a number of impoundments in the continental United States. A critical value  $R_c$  of about 5 to 10 has been suggested so that  $R < R_c$  could be considered a criterion for the presence of reservoir stratification on an annual basis. This implies that a reservoir is stratified on an annual basis only if the detention time (volume discharge) is greater than one or two months. By this indicator most reregulation pools should behave in a vertically unstratified manner with only longitudinal temperature gradients. However, the main reservoirs are generally sufficiently large so that an annual stratification cycle exists. This is demonstrated by Table 1 which contains a compilation of US Army Corps of Engineers data

---

\* A table of factors for converting non-SI units of measurement to SI (metric) units is presented on page 3.

on reservoir-reregulation pool systems. Three of the facilities are used in conjunction with pumped-storage operations. The reregulation pool is generally a small fraction of the volume of the main reservoir for each project. The detention times for the reregulation pools in this table are typically less than 20 days. Therefore, the important gradients are in the vertical direction for the main reservoir, and generally in the longitudinal direction in the reregulation pool.

#### Numerical Description of the Reservoir

11. In order to study the impact of structural or operational modifications on the reservoir temperature distribution and release, numerical models which reproduce the major features of thermal stratification were developed. These models had to be inexpensive so that simulation over the long time periods required to reproduce the stratification cycle of the reservoir would be practical.

12. As a result, the US Army Engineer Waterways Experiment Station (WES) developed a one-dimensional thermal model (WESTEX, based primarily upon the work of Clay and Fruh (1970)) to describe the stratification process. The model impoundment is discretized into horizontal layers which are assumed to be homogeneous. A particular mass of water entering a stratified reservoir has been traced with dye in the field (Elder and Wunderlich 1968, Knight 1965) and found to eventually reside at the vertical location with approximately the same density as the inflow. Therefore, the WESTEX model places the inflow in the layer which is closest in density. The velocity profile, due to outflow from the reservoir, determines the contribution from each layer to the temperature of the release. The profile is determined by a description developed by Bohan and Grace (1973). Edinger and Geyer (1965) and Edinger, Brady, and Geyer (1974) developed a method for defining the heat transfer at the water surface. The method is based on the concept of an equilibrium surface temperature towards which the heat exchange process attempts to adjust. This has been incorporated into WESTEX, together with an exponential absorption of short-wave solar radiation with depth

due to light penetration. The latter is based upon the developments of Dake and Harleman (1966). The model utilizes an extension of molecular diffusion to describe the nature of the internal heat exchange process. Internal mixing is represented by a mixing scheme based on an integral energy model (Ford 1976).

13. Fontane and Bohan (1974) incorporated a second reservoir capability (for simulating the reregulation pool) in WESTEX which is essentially a zero dimensional thermal budget model. This reregulation pool simulator was coupled with the main reservoir through the main reservoir releases and pumpback flow from the reregulation model. The model system continued to operate inexpensively since the modeling procedure allowed many operations (generation, pumpback) to be made in the reregulation simulator with only a single time step per day of the main reservoir simulation. This reregulation model system is applicable only where the assumption of homogeneity (no lateral, longitudinal, or vertical stratification) of the reregulation pool is reasonable. This assumption was based upon physical model studies and field data that in many cases indicated that the reregulation pool was not vertically stratified (Fontane and Bohan 1974, Dortch et al. 1976, Fontane et al. 1977).

14. Not only does the residence time of the reregulation pool affect temperature, but the release flow rate from the pool can affect downstream temperature. Benedict (1980) modeled the Chattahoochee River proposed reregulation pool as a one-dimensional longitudinal model. His model indicated that reregulation would increase the summer temperatures in the reach of the pool but that the higher base flow from the reregulation pool tended to offset this temperature increase downstream.

15. The most striking result of a reregulation pool is the impact upon the main reservoir, if pumpback is used. The effect of pumpback from the reregulation pool upon the stratification cycle of the upper reservoir has been recorded in numerous studies. Many studies have shown that pumpback resulted in a depressed thermocline (Simmons 1976; Oliver, Hudson, and Clayton 1977; Chen and Orlob 1972; Potter, Stevens, and Meyer 1982). The results of studies at the WES (Holland and Dortch

1982, Fontane et al. 1977, Dortch 1981) also indicated that a more homogeneous density profile results in the main reservoir, following the incorporation of pumped-storage operations.

16. A good description of the pumpback entrainment process and its resulting effect upon stratification is given by Roberts (1981). Figure 2 illustrates the phases which he states reduce stratification. A typical summer stratification condition in the reservoir is shown in Figure 2a. Following pumpback into the main reservoir, a buoyant jet (Figure 2b) ascends entraining fluid from the surrounding reservoir. The volume flow rate of the jet therefore increases. The jet then collapses and spreads horizontally.

17. After the pumpback process ceases (Figure 2c), the density current formed by the pumpback jet continues to spread. The resulting density profile will be less stratified, i.e., more nearly uniform (Figure 2d) than previously. The extent of the impact of pumpback

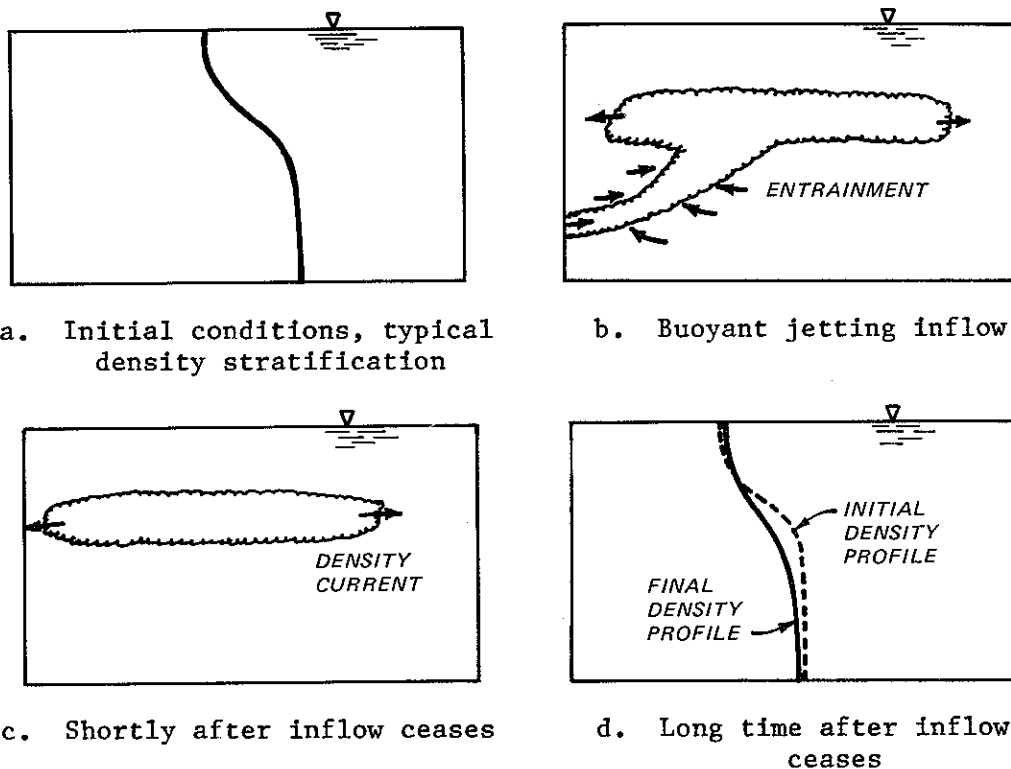


Figure 2. Hydrodynamic features of pumped-storage reservoirs subject to jetting inflows (from Roberts 1981)

entrainment is primarily dependent on the size of the reservoir (a large reservoir being less affected), the rate of the pumpback flow, and the strength of density stratification in the main reservoir.

### Numerical Flow Description for the Reregulation Pool

18. The thermal simulation of a reregulation pool in conjunction with that of the main reservoir needs to be as inexpensive as possible. It would appear that an extension of the WESTEX code for coupling a reregulation pool that can handle longitudinal gradients requires at least a one-dimensional model. The precision and expense of the simulation method hinges upon the manner in which the hydrodynamics (which can involve the solution of two nonlinear partial differential equations) are calculated. If the density driven currents are considered small, then the transport of heat is calculated without being coupled with the hydrodynamics and involves only one linear partial differential equation.

19. The description of the one-dimensional equations of open channel unsteady flow were derived by Saint-Venant (1871). These equations consist of the conservation of mass (continuity) equation:

$$\frac{\partial AV}{\partial x} + \frac{\partial A}{\partial t} = 0 \quad (3)$$

and the conservation of momentum equation (equation of motion):

$$\frac{\partial V}{\partial t} + v \frac{\partial V}{\partial x} + g \left( \frac{\partial h}{\partial x} + S_f \right) = 0 \quad (4)$$

where

A = cross-sectional area

V = velocity

x = distance along the longitudinal axis of the waterway

t = time

$g$  = acceleration of gravity

$h$  = water-surface elevation above datum

$S_f$  = friction slope

20. The solution of the set of partial differential equations requires a numerical procedure which is somewhat laborious. An intermediate approximation uses what is termed hydrologic modeling. These models are based on the conservation of mass equation in the following form (Chow 1959):

$$I - O = \frac{\Delta S}{\Delta t} \quad (5)$$

in which  $\Delta S$  is the change of storage within the reach during a time increment; the storage ( $S$ ) is assumed to be related to inflow ( $I$ ) and/or outflow ( $O$ ).

$$S = K[XI + (1 - X)O] \quad (6)$$

$K$  is a storage constant with dimensions of time (secs), and  $X$  is a weighting coefficient,  $0 \leq X \leq 1$ .

21. Storage routing models attributed to Puls (1928) and Goodrich (1931) were developed assuming  $X$  to be zero. Writing Equation 3 in centered time and space finite difference form yields the following reservoir routing model:

$$\frac{I(t) + I(t + \Delta t)}{2} - \frac{O(t) + O(t + \Delta t)}{2} = \frac{S(t + \Delta t) - S(t)}{\Delta t} \quad (7)$$

This may be used to calculate flow distribution throughout the pool assuming a level pool (Henderson 1966).

22. Solving the actual Saint-Venant equations has been addressed by several numerical approaches, one of the earliest being the characteristic method. The basic method reduces the set of two partial differential equations to a set of four ordinary differential equations by

choosing the  $x$  or the  $t$  increment so that the  $\Delta x/\Delta t$  ratio lies along a characteristic of the original set of partial differential equations. Many of the early characteristic schemes were explicit (only one unknown per equation), such as the schemes of Liggett and Woolhiser (1967), Streeter and Wylie (1967), Lai (1967), and Ellis (1970). Implicit (more than one unknown per equation) characteristic models were reported by Amein (1966) and Wylie (1970).

23. Many finite difference numerical models of the Saint-Venant equations have been reported. In finite differences the partial derivatives are replaced by difference expressions which are approximations. Early work was registered by Stoker (1953) with later models developed by Garrison, Granju, and Price (1969); Liggett and Woolhiser (1967); Martin and De Fazio (1969); Strelkoff (1969); Dronkers (1969); and Johnson (1974). There are of course many variations in the manner in which the differences are formulated. However, all the methods used in the references above suffer stability restrictions which result in small increments of  $t$ . The limitation is roughly that a surface wave cannot move more than one computational cell per time step. As an example, consider an  $x$  increment of 1/2 mile in a channel 30 ft deep. This criterion would limit the time step to about 90 sec. A typical reservoir simulation period is 1 year, and  $3.5 \times 10^5$  time steps would be needed. Therefore, explicit schemes would not be practical for this study.

24. Implicit finite difference schemes solve a system of equations containing more than one unknown per equation for values at each  $X$  grid location per time step. Implicit models were first suggested by Isaacson, Stoker, and Troesch (1956). Many authors have since devised additional implicit schemes, e.g., Preissmann (1961), Baltzer and Lai (1968), Dronkers (1969), Amein and Fang (1970), Fread (1973). These methods can be shown to be unconditionally stable for the linear advection equation.

$$\frac{\partial V}{\partial t} + c \frac{\partial V}{\partial x} = 0 \quad (8)$$

which is an analogy for the Saint-Venant equations.

25. The nonlinear partial differential equations can be approximated as a set of finite difference equations in an implicit fashion with the following approximations suggested by Fread (1973):

$$\frac{\partial K}{\partial t} \approx \frac{K_i^{n+1} + K_{i+1}^{n+1} - K_i^n - K_{i+1}^n}{2\Delta t} \quad (9)$$

$$\frac{\partial K}{\partial x} \approx \frac{\theta(K_{i+1}^{n+1} - K_i^{n+1})}{\Delta x} + \frac{(1 - \theta)(K_{i+1}^n - K_i^n)}{\Delta x} \quad (10)$$

$$K \approx \frac{\theta(K_i^{n+1} + K_{i+1}^{n+1})}{2} + \frac{(1 - \theta)(K_i^n + K_{i+1}^n)}{2} \quad (11)$$

where

$K$  = any function or variable

$\Delta x$  and  $\Delta t$  = space and time increments

$i$  and  $n$  = the mesh  $x$  location and time

$\theta$  = time-weighting factor

The temporal difference is time-space centered and the spatial derivatives and variable representation are space-centered between  $i$  and  $i+1$ . A weighting factor of  $\theta = 1$  yields the fully implicit scheme used by Baltzer and Lai (1968). A weighting factor of  $\theta = 1/2$  produces the time-centered "box" scheme used by Amein (1966), Amein and Fang (1970), and Contractor and Wiggert (1972).

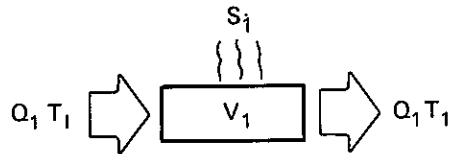
26. Fread (1973) has shown that although the scheme is unconditionally stable for  $\theta \geq 1/2$  for the linear advection equation, nonlinear stability is more limited. Nonlinear stability was found to require  $\theta \geq 0.55$ . Fread found that the closer  $\theta$  is to 0.5, the lower the numerical distortion. Fread (1971) also developed an efficient solution algorithm for solution of the linearized system of equations taking advantage of the banded coefficient matrix.

PART III: METHODS OF ANALYSIS

Analytic Analysis

27. In order to evaluate the limitations and strengths of the candidate simulation methods and demonstrate the potential effects of reregulation upon the transport of a constituent, a progression of simplified models will be considered. In these examples, temperature will be the constituent under consideration; application to a conservative constituent could easily be made in the same fashion.

28. First, consider a single, well-mixed reservoir in which the inflow matches the outflow.



$Q_1$  = inflow and outflow rate

$T_1$  = instantaneous temperature of the reservoir and also the outflow temperature

$T_I$  = inflow temperature

$V_1$  = volume of the reservoir

$S_1$  = source or sink

The rate of heat transfer into and out of the system should equal the rate of change of heat within the volume,  $dV_1 T_1 / dt$ . Since the volume is constant, this becomes  $V_1 (dT_1 / dt)$ . So,  $V_1 (dT_1 / dt) = \text{heat flow rate in} - \text{heat flow rate out} + \text{sources} - \text{sinks}$

$$V_1 \frac{dT_1}{dt} = Q_1 T_I - Q_1 T_1 \pm S_1 \quad (12)$$

or

$$\frac{dT_1}{dt} = \frac{Q_1}{V_1} T_I - \frac{Q_1}{V_1} T_1 \pm \frac{S_1}{V_1} \quad (13)$$

A second reservoir may be considered which is fed by the outflow from reservoir 1. This second reservoir would obviously be represented as

$$\frac{dT_2}{dt} = \frac{Q_1}{V_2} T_1 - \frac{Q_1 T_2}{V_2} \pm \frac{S_2}{V_2} \quad (14)$$

where the subscript 2 represents the second reservoir. If the lower reservoir pumps back into the upper reservoir, this would be a heat flow into the upper and lower reservoirs. In order to keep constant reservoir volumes, the discharges must be redefined. Let  $Q_1$  represent the flow from reservoir 1,  $Q_2$  represent the pumpback rate, and in order to balance the flows, let  $Q_3 = (Q_1 - Q_2) = Q_I$  which will be the net flow into and out of the system. The differential equation for the first reservoir would then be

$$\frac{dT_1}{dt} = \frac{Q_3}{V_1} T_I + \frac{Q_2}{V_1} T_2 - \frac{Q_1}{V_1} T_1 \pm \frac{S_1}{V_1} \quad (15)$$

whereas, the second reservoir would be

$$\frac{dT_2}{dt} = \frac{Q_1}{V_2} T_1 - \frac{Q_3}{V_2} T_2 - \frac{Q_2}{V_2} T_2 \pm \frac{S_2}{V_2} \quad (16)$$

29. Consider a two-reservoir system as shown in Figure 3. Reservoir 1 serves as the major reservoir and reservoir 2 as the reregulation pool. Assuming both reservoirs to be homogeneous (well-mixed), the system of differential equations which describes the heat budget of each reservoir is:

$$\frac{dT_1}{dt} + AT_1 - BT_2 - C = 0 \quad (17)$$

$$\frac{dT_2}{dt} + DT_2 - ET_1 - F = 0 \quad (18)$$

where

$$A = \frac{1}{V_1} \left( Q_1 + \frac{K}{\gamma c_p} A_1 \right)$$

$$B = \frac{Q_2}{V_1}$$

$$C = \frac{1}{V_1} \left( Q_3 T_I + \frac{K}{\gamma c_p} A_1 T_E \right)$$

$$D = \frac{1}{V_2} \left( Q_2 + Q_3 + \frac{K}{\gamma c_p} A_2 \right)$$

$$E = \frac{Q_1}{V_2}$$

$$F = \frac{1}{V_2} \frac{K}{\gamma c_p} A_2 T_E$$

$A_n$  = surface area of reservoir  $n$

$V_n$  = volume of reservoir  $n$

$T_n$  = temperature of reservoir  $n$

$Q_1$  = flow rate in generation (from reservoir 1 to 2)

$Q_2$  = pumpback rate (flow rate from 2 to 1)

$Q_3$  = net flow rate through the entire system, (equal to the inflow to reservoir 1, and also the release from reservoir 2)

$\gamma$  = specific weight of water

$c_p$  = specific heat of water

$n$  = 1 or 2, denoting the main reservoir and reregulation pool, respectively

30. Surface-heat exchange is determined by an approach developed by Edinger and Geyer (1965) and Edinger, Brady, and Geyer (1974). The thermal equation quantifying the net surface-heat exchange (after some linearization) is:

$$H_s = K(T_E - T) \quad (19)$$

where

$H_s$  = net rate of surface-heat transfer

$K$  = coefficient of surface-heat exchange

$T_E$  = equilibrium temperature

$T$  = water-surface temperature

Equilibrium temperature is defined as that temperature at which the net rate of heat exchange between the water surface and the atmosphere is zero.

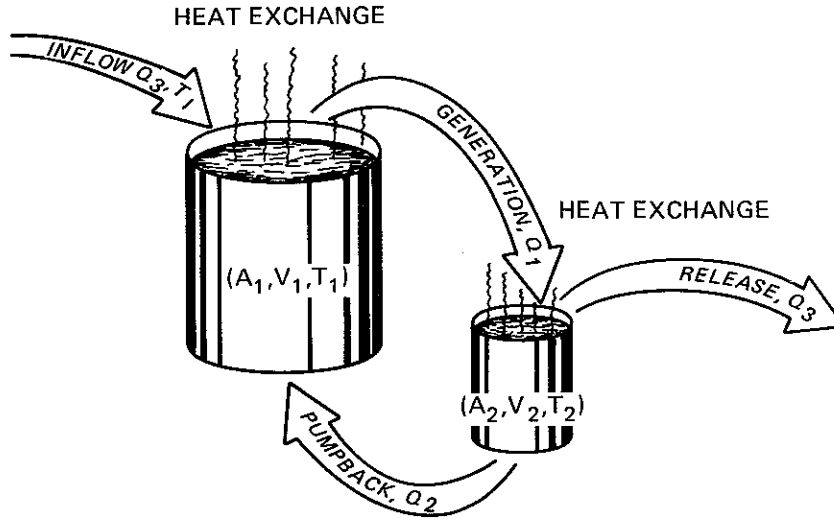


Figure 3. Two-reservoir system with pumpback

31. Assuming that  $V_1$ ,  $V_2$  and  $A_1$ ,  $A_2$  are constants, then  $Q_1 = Q_2 + Q_3$ . The system can then be considered steady-state for flow for certain time frames such as on a daily basis. The general solution of Equations 17 and 18 is:

$$T_1(t) = C_1 e^{M_1 t} + C_2 e^{M_2 t} + \left( \frac{FB + DC}{DA + EB} \right) \quad (20)$$

$$T_2(t) = C_3 e^{M_1 t} + C_4 e^{M_2 t} + \left( \frac{FA + EC}{DA + EB} \right) \quad (21)$$

where

$$C_1 = - \left( \frac{1}{M_2 - M_1} \right) \left[ M_2 \left( \frac{FB + DC}{DA - EB} \right) + C + BT_{2i} - (A + M_2) T_{1i} \right]$$

$$C_2 = \left( \frac{1}{M_2 - M_1} \right) \left[ M_2 \left( \frac{FB + DC}{DA - EB} \right) + C + BT_{2i} - (A + M_1) T_{1i} \right]$$

$$C_3 = - \left( \frac{1}{M_2 - M_1} \right) \left[ M_2 \left( \frac{FA + EC}{DA - EB} \right) + F - (D + M_2) T_{2i} + ET_{1i} \right]$$

$$C_4 = \left( \frac{1}{M_2 - M_1} \right) \left[ M_1 \left( \frac{FA + EC}{DA - EB} \right) + F - (D + M_1) T_{2i} + ET_{1i} \right]$$

$$M_1 = \frac{-(A + D) + \sqrt{(A - D)^2 + 4EB}}{2}$$

$$M_2 = \frac{-(A + D) - \sqrt{(A - D)^2 + 4EB}}{2}$$

$T_{1i}$  = initial temperature of reservoir 1

$T_{2i}$  = initial temperature of reservoir 2

Homogeneous reservoir system, conservative constituents

32. First, consider the condition in which there is no surface-heat exchange. The temperature therefore behaves as a conservative constituent. How does the reregulation pool affect the transport of a constituent? A simple example will be used to illustrate this influence. The example system contains a reregulation pool with an initial temperature,  $T_{2i}$ , equal to the temperature of the inflow to the system,  $T_I$ . The major reservoir (reservoir 1) has an initial temperature,  $T_{1i}$ , 1 deg higher than the initial temperature of the reregulation pool. If the initial reregulation pool temperature is considered a reference temperature (background temperature), then:

$$T_I = 0$$

$$T_{1i} = 1$$

$$T_{2i} = 0$$

These temperatures are only relative temperatures relating the major reservoir and the reregulation pool. The ratio of net flow  $Q_3$  to the

volume of the major reservoir  $V_1$  is  $Q_3/V_1 = 0.1/\text{unit time}$ ; and the volume of the reregulation pool to the major reservoir  $V_2/V_1 = 0.1$ . Figure 4 illustrates the transport of a conservative constituent (temperature in this example) through the two reservoir systems.

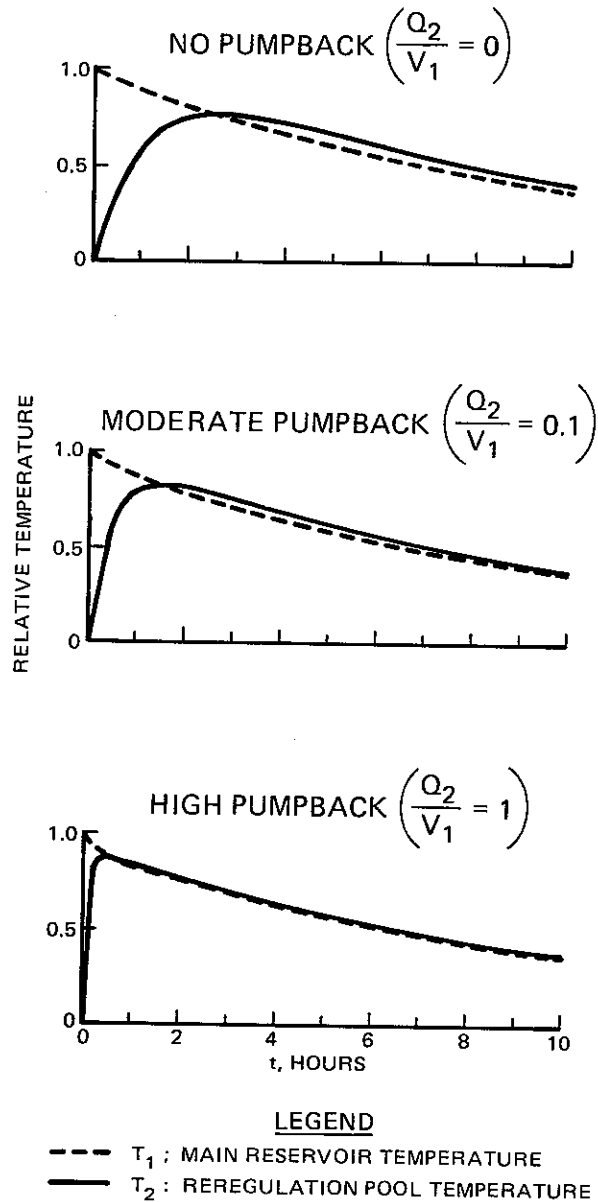


Figure 4. Typical temperature of a two-reservoir system for  $Q_3/V_1 = 0.1$ ,  $V_2/V_1 = 0.1$ , with varying  $Q_2/V_1$  ratios

33. The example shows the temperature time history for the two reservoirs for three levels of pumpback;  $Q_2/V_1 = 0$  ,  $Q_2/V_1 = 0.1$  , and  $Q_2/V_1 = 1$  . The temperature of the major reservoir is, of course, at a maximum initially and is diluted continuously thereafter. The re-regulation pool temperature would rise until it reaches a peak when it is identical to the major reservoir's temperature at that time, after which it also declines. As is illustrated, the peak reregulation pool temperature occurs more quickly as the amount of pumpback is increased. For no pumpback, the time to peak (obtained by setting the time-rate derivative of Equation 21 to zero) is given by:

$$t_p = D \frac{\ln (V_1/V_2)}{Q_1(V_1 - V_2)/V_1V_2} \quad (22)$$

As pumpback increases, the time to peak is reduced, limited by  $t_p = 0$  , of course. In the example,  $t_p = 2.56$  for the no pumpback case; 1.54 for  $Q_2/V_1 = 0.1$  ; and 0.41 for  $Q_2/V_1 = 1$  . The actual peak temperature in the reregulation pool, for this example, increases with increasing pumpback. In this example, the relative peak temperature of the reregulation pool was 0.76 for no pumpback; 0.82 for  $Q_2/V_1 = 0.1$  ; and 0.88 for  $Q_2/V_1 = 1$  . The peak temperature approaches  $(V_1/(V_1 + V_2))T_{1i}$  as pumpback is increased. The larger the pumpback flow rate, the more the two reservoirs behave as if they were a single reservoir which has a volume equal to the sum of the two reservoirs in the system.

34. Figure 5 shows the peak relative temperature and the time to this peak in the reregulation pool as a function of the ratio of reregulation pool volume to major reservoir volume,  $V_2/V_1$  , for  $Q_3/V_1 = 0.1$  . As the relative volume of the reregulation pool is increased, the temperature peak is attenuated. The time to peak temperature increases sharply as the reregulation pool is enlarged. It is evident from Figure 5 that pumpback has negligible impact on the temperature in the system if the reregulation pool is small. Obviously, this applies only in a well-mixed system (no stratification).

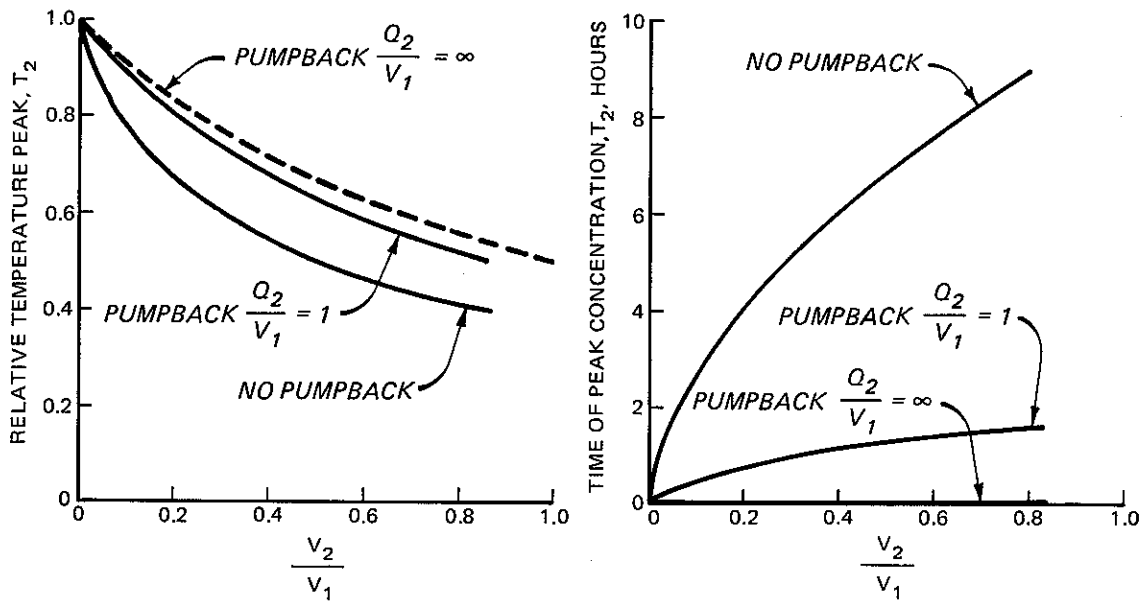


Figure 5. Conservative constituent,  $Q_3/V_1 = 0.1$

Homogeneous reservoir system,  
nonconservative constituents

35. Figure 6 demonstrates the effect of adding surface-heat exchange. For this example the following values of parameters were used:

	<u>Main Reservoir</u>	<u>Reregulation Pool</u>
Volume	300 KAF*	10 KAF
Surface Area	3 KA**	1 KA
Inflow and Release, $Q_3$	0.5 KAF/D†	
Pumpback, $Q_2$	10.0 KAF/D	

\* KAF = kiloacre-feet.

\*\* KA = kiloacre.

† KAF/D = kiloacre-feet/day.

The surface-heat exchange coefficient used in this example was  $K = 140$  BTU/ft<sup>2</sup>-day-°F. The inflow temperature and the initial temperature of the reservoirs were arbitrarily set at 1° F below the equilibrium temperature. This allowed the computation of  $H_s$  as discussed in

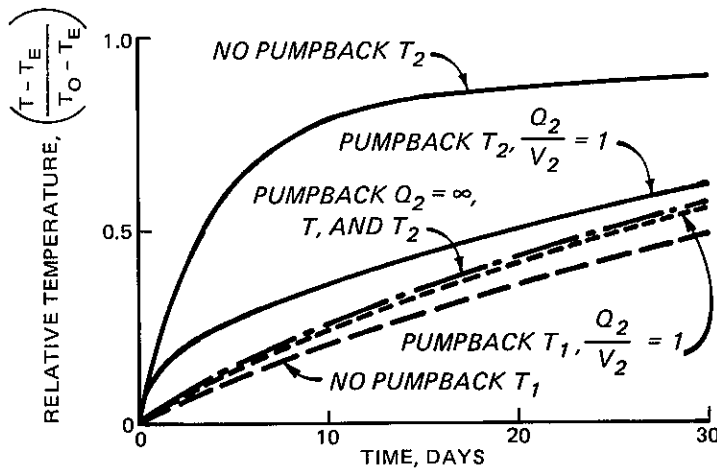


Figure 6. Pumpback effects with heat exchange

paragraphs 27 through 31. In the absence of pumpback, the major reservoir is unaffected by the reregulation pool. While the detention time in the main reservoir is quite large (600 days), its average depth is also large (100 ft), thus the main reservoir heats slowly. The ultimate steady-state temperature for the main reservoir ( $T_{1ss}$ ) under these conditions (from Equation 20 with  $t = \infty$ ) would be given by

$$T_{1ss} = \frac{[Q_3 T_I + K/(\gamma c_p) A_1 T_E]}{[Q_1 + K/(\gamma c_p) A_1]} \quad (23)$$

or 0.930. The rate constant associated with the upper reservoir is  $M_2 = [Q_1 + K/(\gamma c_p) A_1]/V_1 = 0.0241$ . With no pumpback, the rate indicators are  $M_1 = -[Q_1 + (K/\gamma c_p) A_2]/V_2$  and  $M_2 = -[Q_1 + (K/\gamma c_p) A_1]/V_1$ . The magnitudes of  $M_1$  and  $M_2$  are the rate constants associated with the reregulation pool and the main reservoir, respectively. The larger the rate constant, the more rapidly the temperature changes.

36. The rate constant associated with the reregulation pool is substantially larger than that of the main reservoir (0.274 compared with 0.0241), so the reregulation pool is more rapidly influenced by the equilibrium temperature than the main reservoir. Though the reregulation pool cannot influence the main reservoir without pumpback, the

reregulation pool is fed by the upper reservoir so that temperature changes which are produced upstream are built upon by the reregulation pool. The ultimate steady-state temperature of the reregulation pool ( $T_{2ss}$ ) would be

$$T_{2ss} = \frac{\left(\frac{K}{\gamma c_p} A_2 T_E\right) \left(Q_1 + \frac{K}{\gamma c_p} A_1\right) + Q_1 \left(Q_3 T_1 + \frac{K}{\gamma c_p} A_1 T_E\right)}{\left(Q_1 + \frac{K}{\gamma c_p} A_2\right) \left(Q_1 + \frac{K}{\gamma c_p} A_1\right)} \quad (24)$$

For this example, the  $T_{2ss} = 0.987$ . The rate of change of temperature in the reregulation pool is quite rapid compared to the upstream reservoir. Although the detention time in the reregulation pool is only 20 days compared to 600 in the upstream reservoir, the average depth of the reregulation pool is one tenth that of the main reservoir; this, in turn, allows the reregulation pool to have quicker temperature fluctuations than the main reservoir.

37. Figure 6 also shows the effects of pumpback at a rate of 10 KAF/D, where 10 KAF is the volume of the reregulation pool. This rate of pumpback resulted in a substantially different reregulation pool temperature history than that computed for no pumpback. The impact of this pumpback rate on the main reservoir was, however, considerably less than that on the reregulation pool due to the large size of the main reservoir. Again, the pumpback caused mixing of the two reservoirs so that they began to behave as a single reservoir. The temperature history for a pumpback rate  $Q_2 = \infty$  is also shown in this figure. Under this condition,  $T_1 = T_2$ . Since the reregulation pool is much smaller than the main reservoir, the effect of pumpback is more pronounced upon it than upon the larger reservoir. An important feature of this pumpback is that during periods of warming, the reregulation pool will generally warm more quickly than the main reservoir, and the pumpback will tend to heat the main reservoir.

38. The presence of the reregulation pool obviously promotes conditions different from natural conditions within this same reach. The

reregulation dam stores pulses of flow and releases a relatively uniform flow. This storage produces a different response in the reach to the equilibrium temperature fluctuations. Again considering daily average events, analysis of these effects would be quasi-steady state. The system may be described by:

$$\frac{dT}{dt} + \frac{QT}{V} + \frac{KA}{\gamma_c V} (T - \alpha \sin \theta t) = 0 \quad (25)$$

where

T = temperature of the reach

Q = flow through the reach

V = volume of the reach

A = surface area of the reach

$\alpha \sin \theta t$  = equilibrium temperature as a function of time

$\theta$  = cycle frequency =  $2\pi/T_c$

$T_c$  = cycle period

The solution for the case in which the initial temperature of the pool is assumed to be zero (compared to a given reference point) is:

$$T = S\alpha \frac{R \sin \theta t - \theta \cos \theta t}{R^2 + \theta^2} \quad (26)$$

where

$$S = \frac{KA}{\gamma_c V}$$

$$R = \frac{Q + \frac{K}{\gamma_c} A}{V}$$

39. The characteristics of a reach will determine the system's temperature response to the particular heating cycle. If the frequency of the heating cycle is very low (i.e., 1 year), the amplitude ratio of the temperature fluctuation in the pool to that of the environment would then be given by  $(KA/\gamma_c)/[Q + (KA/\gamma_c)]$ . So, if Q is small

compared to the heat exchange component ( $KA/\gamma c_p$ ), the detention time in the reach is long enough for the range of fluctuations of the temperature in the reach to almost match that of the environment. Conversely, a larger discharge through the reach would shrink the temperature range. Thus, the increased surface area associated with the reregulation pool tends to cause greater temperature fluctuations compared to base (no reregulation pool) conditions and in response to low frequency heating cycles. For high frequency loadings, the temperature response would be quite small except for very shallow pools.

40. As an example, consider the previous instance where the pool volume was 10 KAF, the surface area was 1 KA, the discharge was 0.5 KAF/D, and the surface-heat exchange coefficient was 140 BTU/ft<sup>2</sup>-day-°F. Table 2 shows the ratio of the amplitude of temperature fluctuation cycle experienced in the reregulation pool reach to that of the equilibrium temperature for conditions with and without (natural) a reregulation pool. The atmospheric heating cycles which were of primary interest were 1 day and 1 year. These would probably describe the strongest cyclic temperature variations for the reach. This table furnishes information for these two cycles and for a frequency of zero (infinite heating period). The critical factor for the high frequency diurnal heat loading (the 1-day loading period) is the mean depth of the pool (in this example 10 ft). Of course, a small mean depth implies a large surface area for a given pool volume. Even for such a shallow depth, the response of the pool was less than 4 percent of the equilibrium temperature amplitude. The annual cycle produced a response in the pool of 81 percent of the amplitude of the equilibrium temperature. So for all but the shallowest conditions, the daily fluctuations in pool temperatures would be quite small compared to that of the annual cycle for the reregulation pool reach.

41. As shown in Figure 7, a schematized natural flow condition would be within the channel banks, whereas the reregulation pool might often flood areas above this elevation and spill into the natural flood plain. For example, let the natural surface area be 0.25 KA and the volume be 5 KAF. This means the average depth is 20 ft. Compared to a

REREGULATION POOL

NATURAL POOL

Figure 7. Schematized cross section of a reregulation pool



condition with a flooded overbank, this greater depth leads to even less sensitivity to higher frequency heating cycles than computed for the reregulation pool. Column 2 of Table 2 shows that for the diurnal cycle the example natural pool has a temperature range of less than 2 percent of that of the environment. The combination of increased mean depth and a reduction in detention time (resulting from all flow staying in-bank for the natural reach) caused the temperature amplitude in the natural reach to be only 53 percent of the long-period equilibrium temperature cycle amplitude. The reregulation pool produced a temperature range ratio of over 80 percent for this condition. Therefore, the reach in which the example reregulation pool is located would tend to have larger-than-natural annual and diurnal temperature variations due to its increased detention time and surface area.

42. While the reach which contains the reregulation pool may have a greater temperature fluctuation than occurs without the reregulation pool, this is not necessarily the case below the reregulation dam. The primary function of the dam is to store widely varying generation flow and produce a relatively uniform outflow. The extreme low flow conditions which may occur without the reregulation pool during nongeneration periods could allow quicker adjustment of the water temperatures to the equilibrium temperature environment than would the uniform release produced by the reregulation pool. The water would become more acclimated to the equilibrium temperature conditions during nongeneration periods due to the shallower mean depth and decreased velocities than those for analogous periods of higher uniform releases from the reregulation pool. Conversely, during the periods of generation activity with no reregulation pool, the flow would be less acclimated to the temperature of the environment than would be experienced with the lower, albeit uniform reregulation pool release. Thus, in summer or warm season months the

temperature range experienced in the reach below a hydropower facility with no reregulation pool could be quite large due to the wide variation in flow between generation and nongeneration periods. This variation would be lessened somewhat by the uniform nature of reregulation pool outflow.

43. These conclusions are similar to the results described by Benedict (1980) in a modeling effort concerning the proposed Chattahoochee reregulation pool below Buford Dam. Benedict was concerned with a summer heating scenario in which the proposed reregulation pool, as modeled, would increase temperatures in the reach relative to existing conditions. However, flow variations in the reach would be dampened by the reregulation dam so the temperature fluctuations below the dam would be reduced relative to existing conditions. His results showed that the higher base flows provided by the reregulation dam would tend to offset some of the warming caused by the reregulation pool. Zimmerman and Dortch (1986) modeled the Chattahoochee River in an unsteady manner. They found that modeling of the dynamics was essential to register downstream temperature features in addition to those due to higher base flows.

44. The discussion thus far has concerned homogeneous reservoirs. However, potentially the most significant effect of a reregulation pool in a pumped-storage hydropower system will be its effect upon the stratification cycle of the main reservoir. As was previously demonstrated, a large reservoir with a relatively small flow-through has a large detention time and would have a wide temperature variation for long-period heating cycles. This analysis indicates the entire reservoir should get quite warm in the summer and cool in the winter. However, this is not generally the case. In the spring or early summer, heat is transferred into the surface layers more rapidly than it can be diffused or mixed into the subsequent lower layers. Since warm water is less dense than cold water, it tends to rise toward the surface. This action forms a density gradient which effectively inhibits any further mixing. This process results in a density-stratified reservoir.

45. As the cooling season approaches, the upper layers are cooled and thus sink. This action reduces density gradients so that eventually circulation is often produced over the entire depth during the winter; the reservoir subsequently becomes relatively homogeneous. The pumpback into the main reservoir can reduce the stratification in the upper reservoir by both direct and indirect means. The direct manner is due to the mixing and entrainment by the pumpback plume in the main reservoir. The indirect method is due to the return of the warmer water from the reregulation pool causing a further reduction of the density gradient. This return flow from the reregulation pool can drastically modify the stratification cycle of the main reservoir. Thus, the effect of stratification upon the reregulation pool dynamics must be considered. The process is sufficiently complex so that its analysis usually requires modeling.

Summary of reregulation pool effects from analytic analysis

46. The storage associated with a reregulation pool will result in longer detention times than would occur without a reregulation pool. Therefore, the annual-cycle temperature amplitude of waters in the reach could be increased compared to nonrereregulated conditions and result in warmer summer water temperatures in the reach of the pool.

47. Downstream of the reregulation pool, the more uniform flows produced by this pool may moderate short period (diurnal) temperature fluctuations compared to nonrereregulated conditions. The longer-period temperature cycles may also be moderated some distance below the reregulation dam.

48. The response to daily temperature cycles in the reregulation pool reach will generally be slight. The response is primarily dependent on the mean depth; therefore, the diurnal fluctuation in temperature within the reregulation pool may be more or less than the natural fluctuation, depending upon the bathymetry of the pool.

49. In a pumped-storage system, large pumpback rates cause the upper reservoir and reregulation pool to become similar in quality if the upper reservoir and the reregulation pool are homogeneous. During

warming trends the reregulation pool, in conjunction with pumpback operations, will tend to warm the main reservoir more quickly. The concentration of a conservative constituent in the main reservoir will attain the same value in the reregulation pool more quickly with increasing use of pumpback generation. The peak concentration in the reregulation pool will again tend to be higher with greater pumpback and generation.

50. Pumpback into the main reservoir from the reregulation pool can result in considerably more uniform density profiles there. The degree of influence of the entrainment and mixing depend on the relative size of the upper reservoir, the magnitude of pumpback, and the strength of density stratification in the main reservoir.

#### Numerical Modeling Analysis

51. The interchange of water between the upper reservoir and the reregulation pool can have a variety of effects upon the environmental regimen of either pool. As Clugston and Prince (1980) stated: "The severity of the alterations depends on the surface area, depth, and morphometry of both reservoirs; the volumes of water exchanged; water retention time; depth of intake and discharge structures; and season and time of day during which a plant operates." Consequently, a modeling system that has sufficient flexibility and is relatively inexpensive for simulation of long periods of interest is necessary to obtain reliable results for actual investigations. This particular study builds upon previous work conducted at WES in which the thermal model WESTEX was developed and extends the modeling capability associated with simulation of the reregulation pool in tandem with the main reservoir.

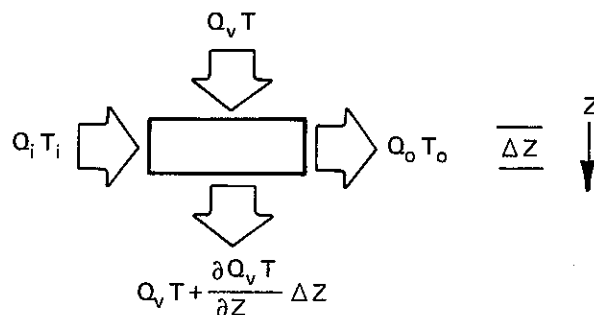
52. The WESTEX model is a one-dimensional numerical model which provides the vertical stratification structure needed to describe hydrodynamic behavior in the main reservoir. This particular modeling effort will concentrate upon the incorporation into the WESTEX model of a numerical one-dimensional (longitudinal) description of the reregulation pool to provide information on longitudinal gradients. A basic

assumption is that the pool is well-mixed vertically and laterally. This assumption seems reasonable, given the short detention times associated with existing reregulation pools. By modeling each reservoir as a one-dimensional system (longitudinal resolution in the reregulation pool and vertical in the main reservoir), the physically significant characteristics of each reservoir will be maintained while keeping computer costs low.

#### Discussion of WESTEX model

53. The basic equation which is solved by WESTEX is the one-dimensional advection-diffusion equation. It relates the increase in heat in an element to the transport of heat by advection or diffusion across the boundaries of the element along with the sources and sinks. This equation is derived as follows:

Advection:



The increase in heat due to vertical advection is

$$\Delta t \left( Q_v T - Q_v T - \frac{\partial Q_v T}{\partial Z} T \Delta Z \right) = \frac{-\partial Q_v T}{\partial Z} \Delta t \Delta z$$

where

$\Delta t$  = the time step length

$Q_v$  = the net vertical flow into or out of a layer

The increase in heat due to inflow and withdrawal is

$$\Delta t (Q_i T_i - Q_o T_o)$$

where

$Q_i$  = inflow rate, cfs/day

$T_i$  = temperature of the inflow, °F

$Q_o$  = withdrawal rate, cfs/day

$T_o$  = temperature of the withdrawal, °F

Dispersion:

The heat transfer is assumed to be described by Fickian diffusion.

Transport through the top of the element is given by

$$-KA \frac{\partial T}{\partial Z} \Delta t$$

Whereas, transport through the bottom of the element is

$$-\left[ KA \frac{\partial T}{\partial Z} + \frac{\partial}{\partial Z} \left( KA \frac{\partial T}{\partial Z} \right) \Delta Z \right] \Delta t$$

Therefore, the heat transfer due to dispersion can be written as

$$\frac{\partial}{\partial Z} \left( KA \frac{\partial T}{\partial Z} \right) \Delta Z \Delta t$$

where

$K$  = vertical diffusion coefficient, ft<sup>2</sup>/day

$A$  = horizontal area of the element, ft<sup>2</sup>

External source:

The increase in heat due to an external source is given by

$$\frac{1}{\rho c_p} \frac{\partial H}{\partial Z} \Delta Z \Delta t$$

where

$\rho$  = density of water, lb/ft<sup>3</sup>

$c_p$  = specific heat of water, BTU/lb/°F

$$\frac{\partial H}{\partial Z} = \text{external heat source, BTU/ft/day}$$

54. The sum of these terms should be the rate of increase of temperature multiplied by the volume of the element control volume

$$A\Delta Z \frac{\partial T}{\partial t} \Delta t ,$$

which then yields the following equation

$$A\Delta Z\Delta t \frac{\partial T}{\partial t} = \Delta t \left[ Q_i T_i - Q_o T_o + \frac{\partial}{\partial Z} \left( KA \frac{\partial T}{\partial Z} \right) \Delta Z - \frac{\partial(Q_v T)}{\partial Z} \Delta Z + \frac{1}{\rho c_p} \frac{\partial H}{\partial Z} \Delta Z \right]$$

Now dividing by  $A\Delta Z\Delta t$  results in

$$\frac{\partial T}{\partial t} = Q_i T_i - Q_o T_o + \frac{1}{A} \frac{\partial}{\partial Z} \left( KA \frac{\partial T}{\partial Z} \right) - \frac{1}{A} \frac{\partial(Q_v T)}{\partial Z} + \frac{1}{\rho c_p A} \frac{\partial H}{\partial Z} \Delta Z \quad (27)$$

This expression for conservation of heat is coupled with the conservation of mass equation for an elemental control volume. The model code was developed with consideration for the long time periods required to simulate the natural stratification cycle of a reservoir. For this reason, a one-dimensional approach was followed. WESTEX was developed at WES but was based upon the prior work of Bohan and Grace (1969, 1973); Clay and Fruh (1970); Edinger and Geyer (1965); Edinger, Brady, and Geyer (1974); and Dake and Harleman (1966). The model includes computational methods for simulating heat transfer at the air-water interface, advective heat transfer of inflow and outflow, and internal dispersion of thermal energy. Since the model is conceptually one-dimensional, the impoundment is divided into discrete horizontal layers of uniform thickness. Fundamental assumptions include the following:

- a. Isotherms are parallel to the water surface.
- b. The water in each discrete layer is isotropic and physically homogeneous.

- c. Internal advection and heat transfer occur only in the vertical direction.
- d. External advection (inflow and outflow) occurs as a uniform distribution within each layer.
- e. Internal dispersion of thermal energy is accomplished by a lumped diffusion mechanism that combines the effects of molecular diffusion, turbulent diffusion, and thermal convection.
- f. There is no heat exchange through the mud-water interface at the bottom.

A description of this model can be found in Holland and Dortch (1982).

55. The WESTEX model has used a sump model to simulate a re-regulation pool. This procedure for reregulation pool (or afterbay) simulation is the approach used in past applications of WESTEX. Its use is documented in several previous investigations (Fontane et al. 1977, Dortch et al. 1976, and Holland and Dortch 1982). The reregulation pool is modeled numerically by maintaining heat and water budgets. Pumpback would logically retrieve some of the water recently entering the afterbay during a generation cycle. This method utilizes a pumpback coefficient which is the percentage of the pumpback water volume that is from the day's generation. The rest of the pumpback amount comes from the afterbay. The remainder of generation volume is then fully mixed with the afterbay. In this manner, some allowance is made to account for longitudinal gradients. However, a single sump system such as this has only a one-day memory since the reregulation pool is fully mixed at the end of each day. The system requires some estimation (through a coefficient) of the percentage of generation flow making up the pumpback volume. The two extremes in this estimation are: (a) plug flow (no longitudinal mixing), where the pumpback volume is made entirely of generated volume and (b) fully mixed, where the pumpback volume is made up of well-mixed reregulation pool quality after generation.

56. Once during each day of simulation the volume of water in the reregulation pool is adjusted to sequentially account for (a) the main reservoir generation volume which is not pumped back; (b) the afterbay volume which is pumped back; and (c) the reregulation pool volume which

is released downstream. The net contributions of the generation volumes from the main reservoir for each operation cycle at their respective temperatures are added to the post pumpback afterbay volume and a volume-weight average temperature for the afterbay is computed. The daily surface-heat exchange is then applied to the afterbay surface area and a new afterbay temperature computed. The temperature of the pumpback volume is computed as a flow-weighted average of the mixed temperatures of the generation volumes pumped back and the percentage of the reregulation pool (at its temperature) which is pumped back.

57. An example of this procedure may illustrate the method more clearly. Consider for example:

- a. A reregulation pool with a volume of 10 KAF and a temperature of 60° F at the beginning of the day.
- b. A generation rate of 10 KAF/D for one-half day which withdraws water of 40° F temperature from the main reservoir.
- c. A pumpback rate of 8 KAF/D for one-half day with a pumpback coefficient of 0.6.
- d. The release rate from the reregulation pool is 1 KAF/D for the entire day.

The volumes added or removed from the reregulation pool are simply the flow rate multiplied by the duration; for this example, 5 KAF for generation, 4 KAF for pumpback, and 1 KAF for the release downstream. The temperature of the pumpback is found by the flow-weighted average temperature of the generation flow returned to the main reservoir (determined by the pumpback coefficient), and the remainder of the pumpback flow which is from the reregulation pool. In this example, the pumpback temperature is given by:

$$\text{Pumpback temperature} = (0.6)(40^\circ \text{ F}) + (0.4)(60^\circ \text{ F}) = 48^\circ \text{ F}$$

Of course, the maximum amount of generation flow which can be returned is limited to that day's generation volume. The temperature and volume of the reregulation pool is then calculated by summation of the flow volume and the flow-weighted temperature of each component of the activities of the day. In this example,

Reregulation pool volume =  $(10 + 5 - 4 - 1)$  KAF = 10 KAF

Reregulation pool volume =  $10$  KAF +  $5$  KAF -  $4$  KAF -  $1$  KAF =  $10$  KAF

Reregulation pool temperature

$$= \frac{[(10\text{KAF})(60^\circ \text{ F}) + (5\text{KAF})(40^\circ \text{ F}) - (4\text{KAF})(48^\circ \text{ F}) - (1\text{KAF})(60^\circ \text{ F})]}{10 \text{ KAF}}$$
$$= 54.8^\circ \text{ F}$$

At this point the surface-heat exchange for the day is applied.

Methods for simulating  
reregulation pools hydrodynamics

58. An alternative to the sump model which provides longitudinal resolution calculates the current velocity and depths by level pool routing and the constituent transport is then calculated by a one-dimensional transport model. As the name implies, in the calculation of hydrodynamic parameters this modeling concept assumes the pool water surface to be level. With this assumption, only the lumped, unsteady continuity equation has to be solved to compute discharge at each cross section. The method proceeds as follows:

a. The total volume of the reregulation pool is found by

$$V_F = V_I + (Q_{in} - Q_{out})\Delta t \quad (28)$$

where

$V_F$  = final volume

$V_I$  = initial volume

$Q_{in}$  = input to reregulation pool (generation)

$Q_{out}$  = outflow from the reregulation pool  
(pumpback and/or downstream release)

$\Delta t$  = time step length

b. From this total volume, the elevation of the pool is interpolated from a table based on the bathymetry of the pool.

c. The change in storage for each longitudinal segment along the pool is found through a table relating the pool elevation with volume for each segment.

- d. The discharge is then calculated at each interior cross section by

$$Q_{i+1} = Q_i - \frac{\Delta S_i}{\Delta t} \quad (29)$$

where

$i$  = cross-section number;  $l = 0$  to number of segments

$Q_i$  = upstream discharge of segment  $i$

$\Delta S_i$  = change in segment  $i$  storage

59. The advantage of this method over the sump method is that it allows longitudinal variation in reregulation pool temperature to be modeled. The temperature and constituent transport is computed by using this discharge distribution in an implicit finite difference transport code to be discussed later.

60. The inclusion of level pool routing exclusive of other hydrologic routing methods was due to its simplicity and its applicability to reregulation pools. It is noted, however, that the resolution of the hydrodynamics concerned with the propagation of the wave surge through the pool for operation changes cannot be determined with this method. However, this may not be necessary to get reasonable constituent and temperature distributions for many problems (such as investigation of hourly or daily average conditions) associated with reregulation pool hydrodynamics.

61. The level pool assumption may be too severe if the width of the pool changes abruptly with water-surface elevation. This would be a problem if the water-surface slope is great enough to result in significant differences in surface area and hence heat exchange along the longitudinal axis of the pool. Impoundments with low velocities would have very slight surface slopes making the assumption of a level pool quite reasonable. As an example, a uniform channel with a velocity of 1 fps and a hydraulic radius of 20 ft would have a friction slope of about  $7.5 \times 10^{-6}$  for a relatively high Manning's  $n$  of 0.03. This is less than 0.04 ft per mile. Thus, even at this velocity and Manning's  $n$ ,

the mildness of the computed friction slope adds validity to the level pool assumption.

62. Another alternative involves solution of the Saint-Venant equations for the velocity currents and depths. For completeness, a derivation of these equations similar to that of Fread (1983) is included in Appendix A. In conservation form the continuity equation is:

$$\frac{\partial Q}{\partial x} + \frac{\partial A}{\partial t} = 0 \quad (30)$$

The momentum equation is:

$$\frac{\partial Q}{\partial t} + \frac{\partial(Q^2/A)}{\partial x} + gA \frac{\partial h}{\partial x} + S_f = 0 \quad (31)$$

where

$$S_f = \frac{n^2 Q |Q|}{2.21A^2 R^{4/3}}$$

A = cross-sectional area

g = acceleration of gravity

h = water-surface elevation

$S_f$  = friction slope

Q = discharge

R = hydraulic radius

x = distance along the waterway

t = time

n = Manning's n

63. The dynamic routing method is the most rigorous of the methods presented. Water-surface elevations and discharge at each cross section are calculated from the continuity and momentum equations of the Saint-Venant equations.

64. The numerical hydrodynamic code developed for this investigation is based upon the modeling work of Fread (1978, 1980). The model

is an implicit finite difference solution of the Saint-Venant equations. The development of the finite difference formulation uses a four-point method in which a time-weighted spatial derivative and a space-centered temporal derivative is employed. The details of the solution method are presented in Appendix B.

65. The implicitness of the solution technique allows for the relatively large time steps which may be needed for simulating the long time periods associated with the stratification cycle of a reservoir. The model accepts a discharge boundary upstream (release from the reservoir or pumpback) and a discharge or a discharge-head relationship for the downstream boundary.

Alternative method for simulating reregulation pool transport

66. The representation of the reregulation pool as a single element is a poor representation for long narrow pools. The release temperatures are simulated as a pool average which makes the response to climatic changes very slow. As an example, consider a long narrow channel with a rectangular cross section. The linear advection diffusion equation with surface-heat exchange can be derived in the same manner as Equation 27 and written as

$$\frac{\partial T}{\partial t} + U \frac{\partial T}{\partial x} - E_L \frac{\partial^2 T}{\partial x^2} = \frac{K(T_E - T)}{D\gamma c_p} \quad (32)$$

where

- U = constant, channel velocity
- $E_L$  = longitudinal dispersion coefficient
- $T_E$  = the equilibrium temperature
- D = the channel depth of flow

A large flow rate in a long narrow pool renders the dispersion term insignificant compared to the advective term. For the purpose of example, consider the initial pool temperature to be the equilibrium temperature and the temperature of the inflow to the pool to be a

constant 1° F above the equilibrium.  $T_E$  may then be subtracted from  $T$  and the partial differential equation redefined as:

$$\frac{\partial T}{\partial t} + U \frac{\partial T}{\partial x} = - \frac{KT}{D\gamma c_p} \quad (33)$$

where the second order dispersion has been neglected. The solution to this equation is

$$T(t) = T_0 (x - Ut) e^{-\frac{K}{\gamma c_p D} \frac{x}{U}} \quad (34)$$

where  $L$  is the length of the pool. To calculate the release temperature, set

$$t = \frac{L}{U} = \frac{BDL}{BDU} = \frac{V}{Q}$$

where

$B$  = width

$V$  = pool volume

$Q$  = discharge

since the temperature at the outflow is reached at this time  $t$  after initiation.  $T_0$  at the upstream end of the pool is a constant 1° F, therefore

$$T = e^{-\frac{K}{\gamma c_p D} \frac{V}{Q}} \quad (35)$$

Choosing,

$$K = 140 \text{ BTU/ft}^2\text{-D-}^\circ\text{F}$$

$$\gamma = 62.4 \text{ lb/ft}^3$$

$$c_p = 1.0 \text{ BTU/lb-}^\circ\text{F}$$

D = 20 ft  
V = 10 KAF  
Q = 10 KAF/D

results in the solution to Equation 32

$$T = 0.899^\circ \text{ F}$$

This temperature at the outflow requires a time of  $t = V/Q = 1$  day for the analytic solution. The simulation as a pool with no longitudinal resolution in a manner similar to the sump method previously used with WESTEX results in the following solution, from Equation 20:

$$T(t) = \left( \frac{QT_o}{Q + \frac{K}{\gamma c_p} A} \right) \left[ 1 - e^{-\left( \frac{Q}{V} + \frac{KA}{\gamma c_p V} \right) t} \right] + 1 \left[ e^{-\left( \frac{Q_1}{V_1} + \frac{KA}{\gamma c_p V} \right) t} \right]$$

or

$$T(t) = 0.899 \left[ 1 - e^{-(1.112)t} \right]$$

which results in the following tabulation:

<u>t, days</u>	<u>T</u>
1	0.603
2	0.802
4	0.889
8	0.899
$\infty$	0.899

The release temperature predicted by the sump method will therefore change too slowly for fluctuations in flow temperature and equilibrium temperature. It is apparent that an improvement of the modeling method to allow for longitudinal resolution in the reregulation pool is needed.

67. The formulation of the constituent transport model used in conjunction with hydrodynamic information and contributed from the level pool routing or the Saint-Venant formulation is based upon the advection-diffusion equation discussed in paragraph 66, but written for a nonrectangular channel, i.e.,

$$\frac{\partial C}{\partial t} + \frac{1}{A} \frac{\partial(QC)}{\partial x} = \frac{1}{A} \frac{\partial(AE_L \frac{\partial C}{\partial x})}{\partial x} \pm S \quad (36)$$

where

- C = constituent concentration
- t = time
- A = cross-sectional area at a given longitudinal location
- Q = discharge through A
- x = longitudinal distance
- $E_L$  = longitudinal dispersion coefficient
- S = sources and sinks for the given constituent

The solution is provided by an implicit finite difference method which is first-order accurate in both time and space. A donor cell arrangement is used for the advective ( $\partial QC/\partial x$ ) term. Again, as in the hydrodynamic portions of the code, the implicit formulation provides less restrictive time step criteria than an explicit methodology.

68. The surface-heat transfer process (the predominate source and sink terms for temperature) is solved by the same basic method in the reregulation pool and the reservoir models except for one difference. In the upper layers, the vertical distribution of heat is not simulated in the reregulation pool model. The process uses the approach developed by Edinger, Brady, and Geyer (1974), as discussed in paragraphs 27 through 31 which deal with analytic analysis, with the exception that the surface temperature is assigned to be the temperature of the particular longitudinal segment. The computation of equilibrium temperature is based solely upon meteorological data as outlined by Edinger, Duttweiler, and Geyer (1968). The thrust of this effort is in selection

of an appropriate method to supply the hydrodynamics (water depths and current velocities), therefore less detail is given here for the transport scheme. However, a more complete documentation of this transport formulation is given in Appendix C.

PART IV: NUMERICAL COMPARISON OF METHODS

Description of Tests

69. To determine the adequacy of the modeling methods, an example of a previous study at WES was rerun for limited conditions. The advantage of using a previous study was that calibration parameters were already known. The study chosen was the investigation by Holland and Dortch (1982) of the proposed reregulation pool for Norfolk Lake, Arkansas. The proposed reregulation facility is one-dimensional in appearance. The afterbay, as previously modeled, had a volume of 12,600 acre-ft and covered an area of 470 acres at maximum pool. Norfolk Lake itself impounds 1,295,700 acre-ft and covers 22,620 acres at the top of the April-to-September conservation pool, el 554 ft, National Geodetic Vertical Datum (NGVD). The proposed reregulation pool was to be about 3.5 miles long which resulted in the use of a worst-case condition of a plug flow formulation in the sump method in this and the previous study. The bathymetry used in this investigation is shown in Figure 8.

70. The proposed project was to be used for pumped-storage, so the impacts of the various methods upon the simulation of stratification

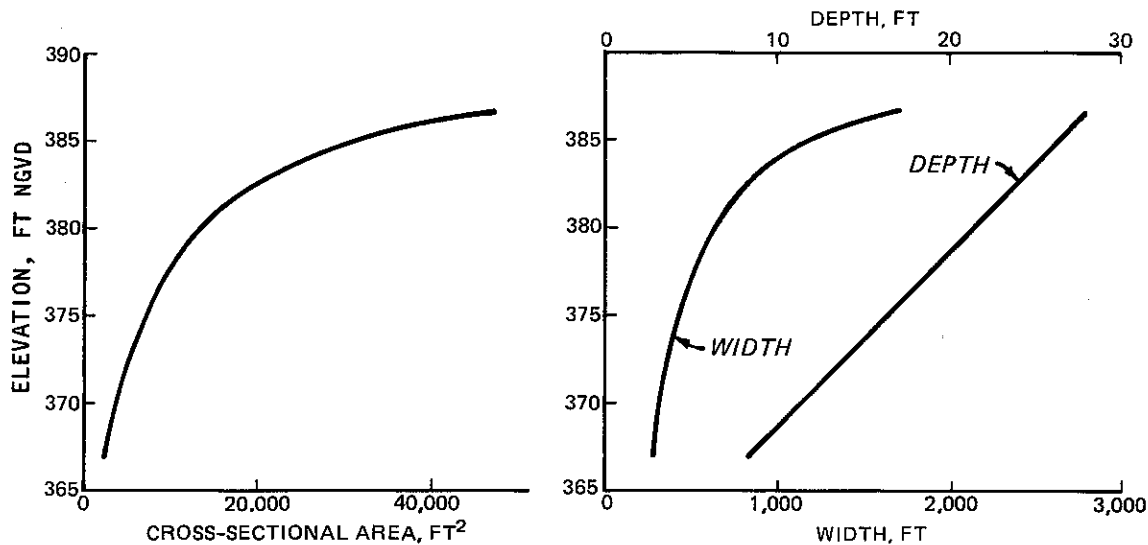


Figure 8. Assumed bathymetry for Norfolk Reregulation Pool

of the upstream reservoir as well as the release from the afterbay may be compared. Figure 9 reviews the schedule of inflow, release, generation, and pumpback rates that were simulated. The pumpback occurred during the stratification season, beginning about day 150 (30 April). A description of the modeling procedure for entrainment and parameters for modeling the upper reservoir are given in Holland and Dortch (1982).

71. The one-dimensional methods utilized a discretization of 10 segments. The Manning's  $n$  roughness criteria, used in the Saint-Venant equations, was set at 0.03. The time step used for both the Saint-Venant and level pool methods was chosen as 1 hr. A separate run

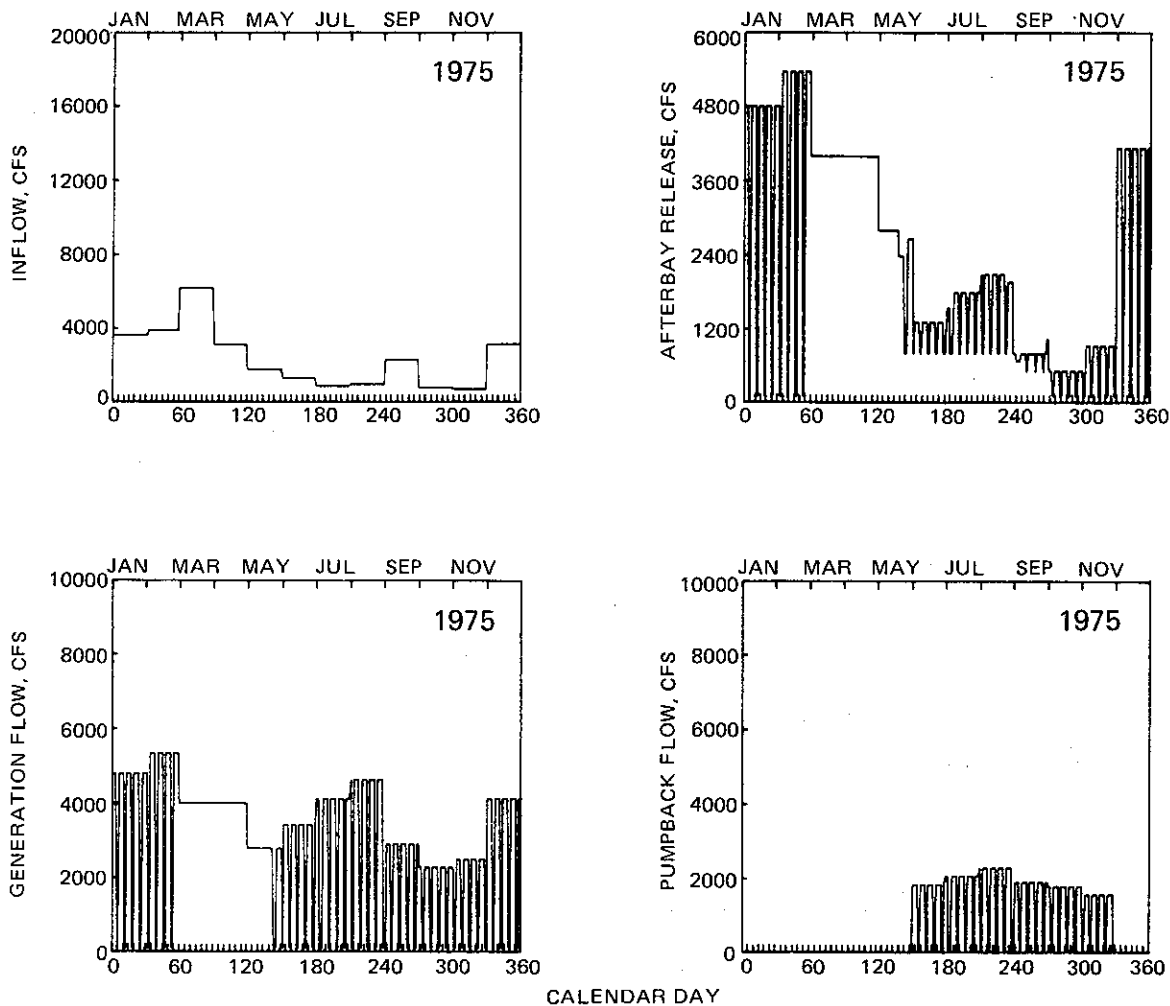


Figure 9. Hydraulic flow boundary information for 1975 representative condition for Norfolk Lake

using the Saint-Venant method was made using a time step of 15 min. The results were nearly identical to those using the 1-hr time step length. So, all subsequent comparisons were made with 1-hr time steps. The dispersion coefficient,  $E_L$ , was estimated to be about  $2 \text{ ft}^2/\text{sec}$  based upon the work of Elder (1959). The remaining parameters for entrainment, heat exchange, etc. were the same for all three schemes and were identical to those developed and used by Holland and Dortch (1982) during the previous study.

### Results

72. The results of the simulation of reregulation pool release temperatures for each of the three methods are shown in Figure 10. The sump method showed average daily release temperatures to vary from about  $7^\circ \text{C}$  in late winter to almost  $18.5^\circ \text{C}$  in the fall. The equilibrium temperatures are periodically registered on the plot as well. The sump

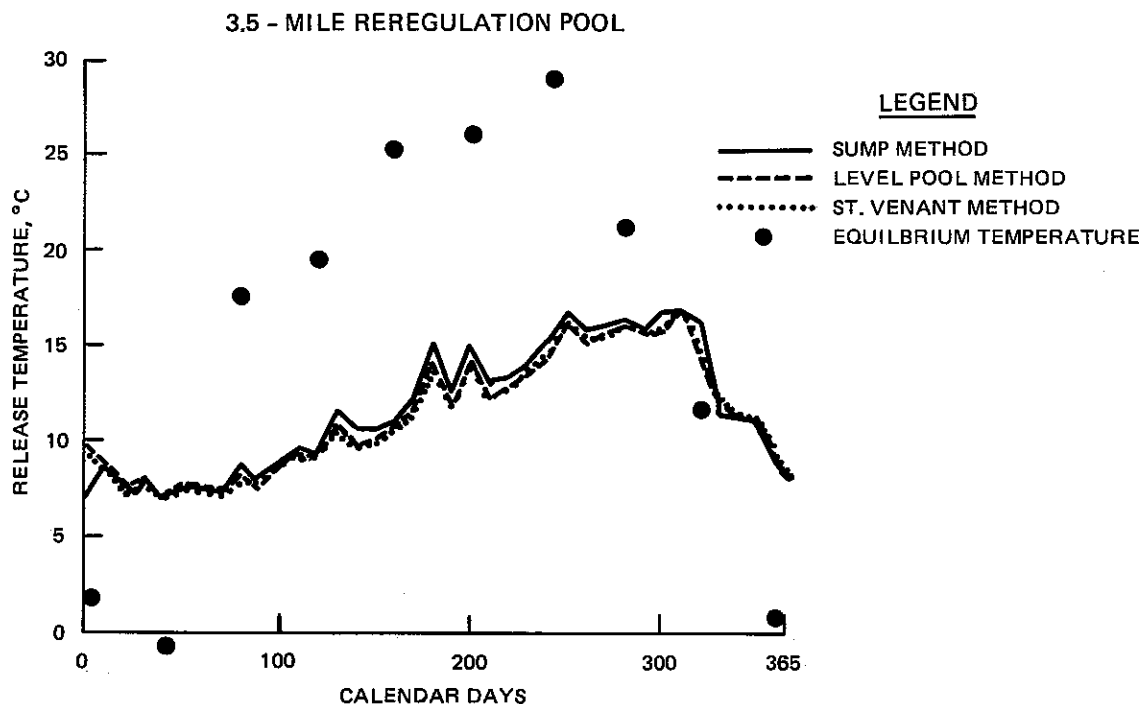


Figure 10. Release temperatures from the proposed Norfolk Reregulation Pool

method mixes the net volume of flow generated upstream with the reregulation pool so that the entire pool is at one temperature. With this method, the sump should respond very slowly to temperature fluctuations. For the other two methods, the reregulation pool can develop longitudinal gradients so that the water leaving the system during warm weather will have had more time to heat (or cool depending on the time of year) than would water that had just reached the center of the pool. Therefore, the longitudinal segmenting allows the model release temperatures to be more strongly influenced by the environmental conditions. However, the sump method in this figure in fact responds quite quickly to changes in equilibrium temperature. It compares well with the other methods for this case. The reason that the comparison is good for the sump method here is two-fold: first, the reregulation pool is relatively small and the detention time is only about 1 day, and second, the use of the pumpback coefficient has a strong influence on the release temperature. Low pumpback coefficients mix the bulk of the generation volume with the reregulation pool so the release temperatures will respond slowly to climate changes. Very high pumpback coefficients return the generation flow, thus providing less mixing with the reregulation pool and allowing the predicted release temperatures to change quickly with climate change. Unfortunately, the pumpback coefficients, while improving the temperature estimate for release, could in fact provide poor temperature prediction in the reregulation pool.

73. Two of the main reservoir temperature profiles computed during the period of the greatest stratification, July 9 and September 18, are shown in Figure 11. The predicted temperature profile for July 9 using the sump method for the afterbay produced temperatures between 9° and 29° C. The level pool results produced a temperature profile quite close to that computed with the sump method. For this reason, the level pool and the Saint-Venant profile results were plotted as deviations from the sump method profile. The middepth layers of the upper reservoir for both one-dimensional methods for modeling the reregulation pool were not as warm as predicted by the sump method. The difference was as much as 0.3° C. The Saint-Venant method resulted in a slightly colder

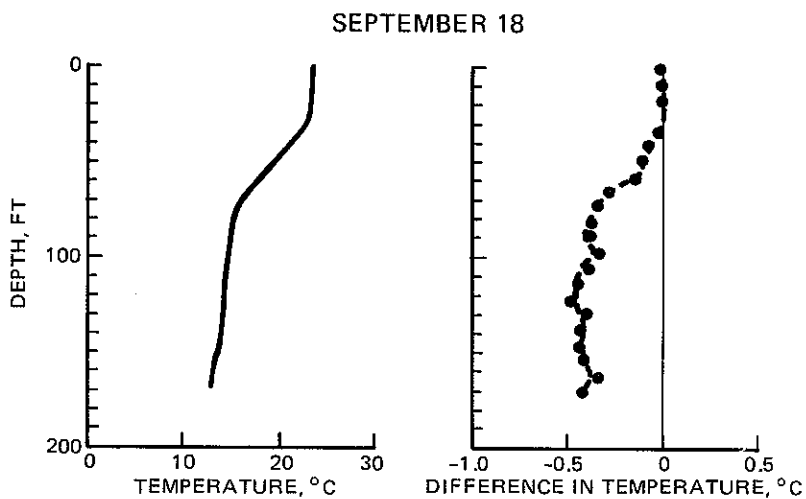
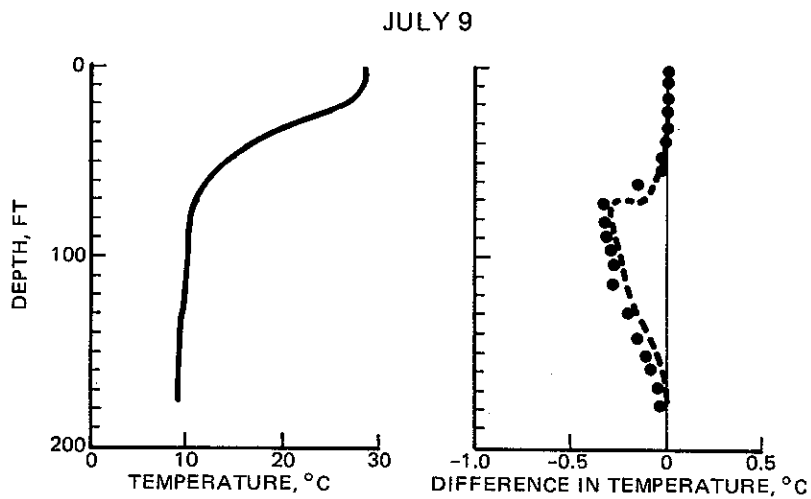


Figure 11. Upper reservoir temperature, Norfolk Lake results

profile than the level pool method by roughly  $0.05^{\circ}\text{C}$ .

74. The September 18 profiles continued in the same manner with the one-dimensional methods predicting more stratification in the main reservoir than the sump method. The sump method produced a temperature

profile in the upper reservoir which ranged between 13° and 22.5° C. The one-dimensional methods produced predicted hypolimnion temperatures which were as much as 0.5° C cooler. The two one-dimensional methods (level pool and Saint-Venant) predicted nearly identical profiles.

75. It seems apparent that the sump method, which has only one compartment to represent the reregulation pool and can only distinguish that day's generation water quality, is lacking in many instances. Further, the pumpback coefficient which is critical to this method is somewhat tenuous to determine. The pumpback temperatures predicted on July 9 were 11.4° and 10.7° C for the sump and the Saint-Venant simulations, respectively. The pumpback temperatures predicted for September 18 were 15.4° and 15.0° C for these two methods. The difference could be reduced by increasing the pumpback coefficient. This would also make the comparison between reregulation pool release temperatures and main reservoir stratification patterns closer. The one-dimensional methods have the added flexibility of many segments to represent the reregulation pool. The primary difference between the one-dimensional methods results from the friction slope causing different water-level predictions in the two methods. This water-level difference can allow different surface-heat exchange due to a difference in surface area. With the relatively short reregulation pool in this example (3.5 miles, the majority of the reregulation pools in Table 1 are shorter than the distance), the water-level differences were not substantial and the results were nearly identical for the level pool and the Saint-Venant methods.

76. In order to investigate potential differences in the one-dimensional methods, the length of the reregulation pool was increased by five times (17.5 miles) and the 1-year simulation rerun. This change should indicate the magnitude of the difference to be expected between results from the level pool and the Saint-Venant method results. The upper reservoir temperature profiles for July 9 and September 18 dates are shown in Figure 12. The temperatures of the metalimnion and hypolimnion for both dates were as much as 0.6° C warmer as predicted with hydrodynamics supplied by the Saint-Venant method compared with level

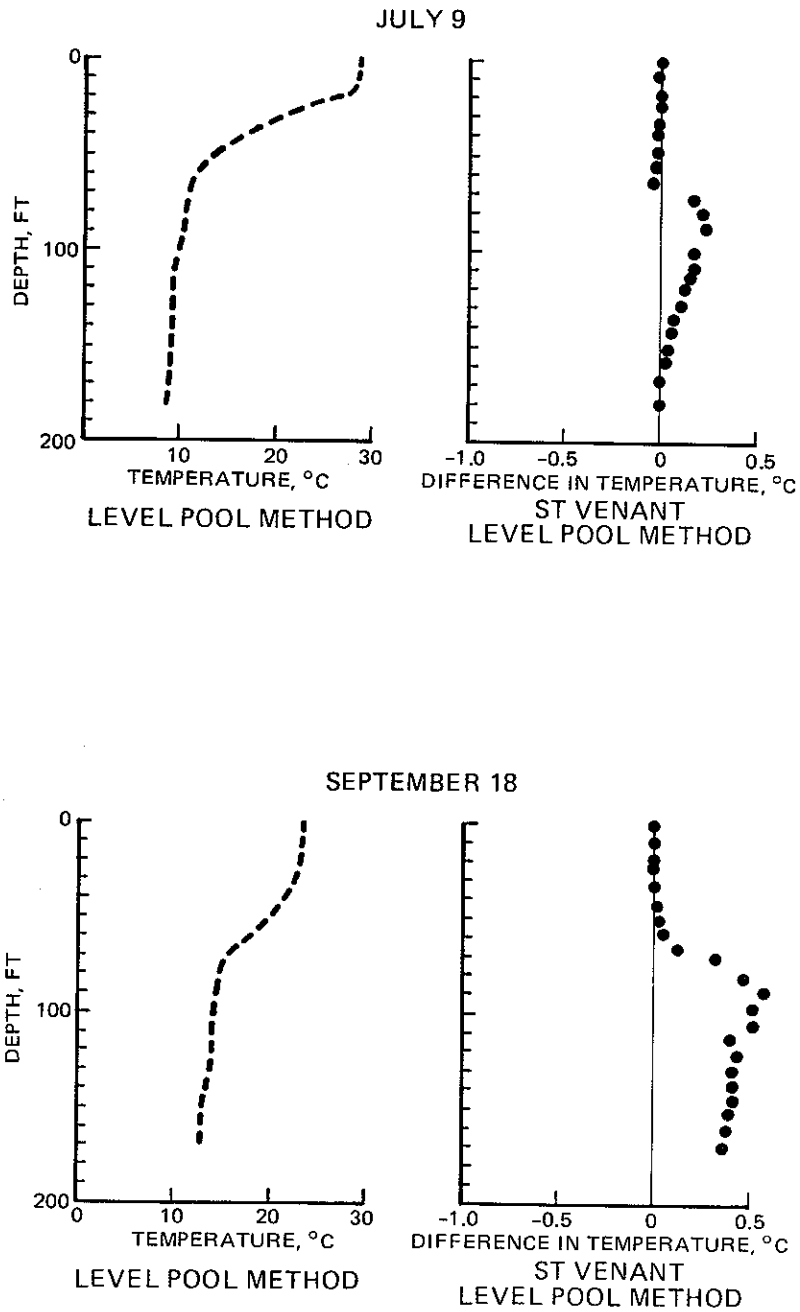


Figure 12. Temperature profiles in the main reservoir for a 17.5-mile-long reregulation pool

pool routing. The release temperatures for these two methods are shown in Figure 13. Again, the temperatures predicted by the Saint-Venant method were warmer by about  $1^{\circ}$  C. The overall comparison between the two methods was quite close with over 99 percent of the variance

explained. The differences in the relative temperatures from the level pool to Saint-Venant simulations are a function of channel slope, the channel cross-section geometry, and the channel roughness. For the same volume, the average depth may be increased or decreased by the level pool assumption relative to the Saint-Venant results. This, in turn, affects the rate of heat exchange through the water surface. Further, the Manning's  $n$  roughness factor used in the Saint-Venant simulation is a calibration parameter which is estimated. In this case, the simulation used a value of 0.030 which is probably somewhat high for a straight prismatic channel. As a sensitivity check, the year simulation was rerun with a Manning's  $n$  value of 0.015. The results are included in Figure 13 for release temperatures. These results were quite close (the level pool method was less than  $0.2^{\circ}\text{C}$  lower on average) to those of level pool routing, even for this relatively long, shallow and narrow reregulation pool.

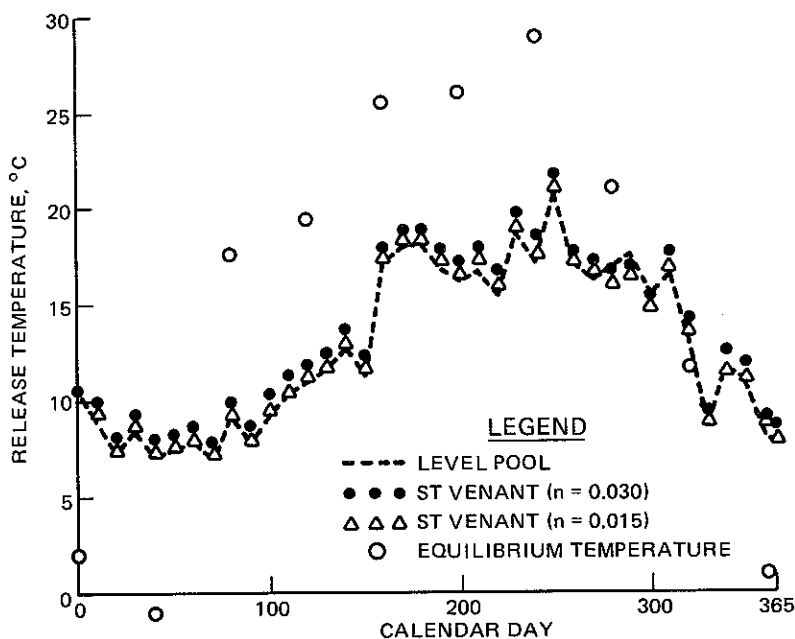


Figure 13. Release temperature from the 17.5-mile-long reregulation pool

## Discussion

77. The Saint-Venant simulations often proved to be difficult to run. These difficulties arose as a direct result of boundary conditions which are typical of reservoir/reregulation pool modeling. Instead of the usual riverine-type boundary conditions, in which the discharge is given upstream and water levels or a stage-discharge relationship downstream, discharge is most often known both upstream and downstream with no water-level information known at either location for the case of interest. This causes problems in conserving mass, due to computational roundoff and precision. This problem is magnified by the long simulation periods required. The problem may be demonstrated by considering a situation in which a discharge  $Q$  enters the basin for 12 hr (with no reregulation outflow) and leaves the basin (with no additional inflow) at the same rate for the next 12 hr. The water volume at the beginning and end of the day should be identical. However, as one computationally steps through the day, calculating the discharge distribution in the basin and the water elevation by the equations of continuity and momentum and the bathymetric tables, the volume at the end of the day will not precisely match that at the day's beginning. After a year of simulation, this could amount to 20 ft or more. The long periods used in reservoir investigations cause this to be a significant problem. This problem was alleviated to some degree by a small convergence criterion (flow rate within 0.1 percent, and water-surface elevation less than 0.005 ft) and additional coding which checks the basin volume after each operation cycle and makes small flow corrections to prod the calculations toward more precise conservation of mass.

78. The level pool method gave results which were comparable to the more elaborate Saint-Venant results, even for the relatively long narrow case of this reregulation pool. The WESTEX code using the level pool routing required only a third the processor time that the WESTEX code using the Saint-Venant scenario required. The Saint-Venant solution does not lend itself well to the particular boundary conditions associated with reservoir simulations.

79. The three methods considered for simulation of hydrodynamics which drive a transport simulation were the sump method, level pool routing, and modeling using the finite difference representation of the Saint-Venant equations. These methods were compared by simulation of a previous study of the proposed reregulation pool at Norfork Reservoir, Arkansas. As the proposed facility was to provide pumped-storage capability for the project, release temperatures as well as the vertical temperature distribution in the main reservoir were compared for each modeling method. The reregulation pool simulation methods were coupled with the vertical one-dimensional thermal model WESTEX to simulate the upper reservoir.

80. An analytical comparison of the sump method with the other two methods demonstrated that the lack of resolution in the reregulation pool with the sump method resulted in a slow response time for predicted release temperatures. If pumpback is being used at the site, a pumpback coefficient improves the prediction of release temperatures. The effect of pumpback, as predicted by the sump method, was less stratification in the upper reservoir during the stratification season than that predicted by the other two methods. The ability of the sump method to produce reliable results depends upon the selection of a pumpback coefficient that generally requires field or physical model input. The need for this coefficient is again caused by the lack of resolution of the sump method. This pumpback coefficient determines the amount of the previous generation flow for a particular day which is returned to the main reservoir during the day's pumpback. With proper resolution this would be determined automatically.

81. The length of the pool for which these comparisons were made was 3.5 miles. However, even for this relatively long, narrow pool, there was essentially no difference between the predictions for the vertical upper reservoir temperature profiles and the release temperatures from the reregulation pool made using level pool routing and the full Saint-Venant equations. A hypothetical reregulation pool 17.5 miles long, with the same widths and cross-sectional areas as previously modeled, was simulated with these two methods. The results

showed some differences between predicted release temperatures for the two one-dimensional methods. However, these differences were so small as to be masked by the estimate of Manning's  $n$  in the Saint-Venant simulations.

82. The finite difference formulation of the Saint-Venant equations also suffered difficulties in the form of lack of conservation of mass with the specified upstream and downstream discharge boundary conditions typical of reservoir modeling. The conservation of mass problems were due to the imprecision of calculations and interpolation of the elevation/volume tables and the long time periods of simulation, resulting in poor conservation of mass. Additional coding reduced the problem by making small corrections to the given flow rates to account for the error in volume in the reregulation pool.

## PART V: SUMMARY AND CONCLUSIONS

### Summary

83. A reregulation dam is used to moderate flow fluctuations due to reservoir releases, often as a result of hydropower operations. The pool formed by the reregulation dam can also serve as the water volume used for pumpback in a pumped-storage generation system. The reregulation pool will impact the temperature of the reservoir-reregulation pool system and the downstream releases. A cost-effective method for simulating the hydrodynamics and heat transport were presented. The method was coupled with a vertical one-dimensional reservoir model to simulate the hydrodynamics and heat transport of the reservoir-reregulation pool system.

84. The modeling procedure for simulating the hydrodynamics and heat transport of the reregulation pool was selected from three candidate methods. The three methods in progressive order of complexity are: (a) the sump method, (b) the level pool routing method, and (c) the finite difference simulation of the Saint-Venant equations. The methods were incorporated within the WESTEX model and the predicted temperature profiles in the main reservoir, and the release temperatures from the reregulation pool were compared to results from the Norfolk Lake study previously conducted at WES.

### Conclusions

85. As demonstrated by the analytic descriptions, the resulting conclusions are given below.

- a. The increased detention time provided by a reregulation pool will result in an increased warm-season temperature in the reach in which the pool is placed. The pool is generally sufficiently deep that short-period fluctuations, such as the diurnal temperature range, will not be significant.

- b. The more uniform flow leaving the reregulation pool will result in a moderation of water temperature fluctuations downstream of the reregulation dam, compared with conditions without the pool.
- c. A pumped-storage system causes a two-way interaction between the major reservoir and the reregulation pool. An analysis of a homogeneous system demonstrates that the similarity of conditions in the upper reservoir and the reregulation pool increases with increasing amounts of pumpback. A conservative constituent found in the main reservoir will reach its peak concentration in the reregulation pool sooner and with a higher concentration for increasing generation/pumpback flows between two homogeneous reservoirs.
- d. The entrainment and mixing processes associated with pumpback will result in a more uniform density profile in the upper reservoir than that observed without pumpback. The degree of influence of the entrainment and mixing is dependent upon the relative size of the reservoir, the rate of pumpback flow, and the density structure of the upper reservoir.
- e. The complexity of geometric description and the physical processes makes modeling necessary when investigating the effects of a reservoir-reregulation pool system. The time period necessary for this simulation is that of the natural stratification cycle, which is generally a year. An efficient simulation routine for such a long period should be used to minimize computational costs.
- f. The very large detention times in the upper reservoir and the small detention times of the existing reregulation pools, as well as historical modeling practice, suggest that resolution of vertical stratification patterns is critical in the upper reservoir while longitudinal gradients are of most importance in the reregulation pool.

86. The results of these simulations indicated that the level pool method was generally the most efficient modeling method of the three. It provided sufficient resolution, was easier to run, was less expensive, and supplied results comparable to the more sophisticated Saint-Venant method. The sump method requires the determination of a pumpback coefficient to provide good comparison of release temperatures. In the event that pumpback is not used, the prediction of release temperatures will change slowly. The Saint-Venant method appears to be needed only if there is a substantial water-surface slope, if the flow

conditions are very dynamic for significant periods of the time domain,  
or if the reservoir is very long.

## REFERENCES

- Amein, M. 1966. "Streamflow Routing on Computer Characteristics," Water Resources Research, Vol 2, No. 1, pp 123-130.
- Amein, M., and Fang, C. S. 1970. "Implicit Flood Routing in Natural Channels," Journal, Hydraulics Division, American Society of Civil Engineers, Vol 96, No. HY12, pp 2481-2500.
- Baltzer, R. A., and Lai, C. 1968. "Computer Simulation of Unsteady Flow in Waterways," Journal, Hydraulics Division, American Society of Civil Engineers, Vol 94, No. HY4, pp 1083-1117.
- Benedict, B. A. 1980. "Review of Expected Water Temperatures Downstream of Proposed Reregulation Dam on Chattahoochee River," Draft Report for US Army Engineer District, Savannah, Savannah, Ga.
- Bohan, J. P., and Grace, J. L., Jr. 1969 (Jul). "Mechanics of Flow from Stratified Reservoirs in the Interest of Water Quality; Hydraulic Laboratory Investigation," Technical Report H-69-10, US Army Engineer Waterways Experiment Station, Vicksburg, Miss.
- \_\_\_\_\_. 1973 (Mar). "Selective Withdrawal from Man-Made Lakes; Hydraulic Laboratory Investigation," Technical Report H-73-4, US Army Engineer Waterways Experiment Station, Vicksburg, Miss.
- Chen, C. W., and Orlob, G. T. 1972(Jun). "Predicting Quality Effects of Pumped Storage," Journal, Power Division, American Society of Civil Engineers, No. P01, pp 65-72.
- Chow, V. T. 1959. Open-Channel Hydraulics, McGraw-Hill, New York.
- Clay, H. M., Jr., and Fruh, E. G. 1970. "Selective Withdrawal at Lake Livingston; An Impoundment Water Quality Model Emphasizing Selective Withdrawal," Progress Report EHE 70-18 (CRWR 66), Environmental Health Engineering Research Laboratory, University of Texas, Austin, Tex.
- Clugston, J. P., and Prince, E. D. 1980. "Pumped Storage Development in the Southwest and Its Effect on Aquatic Environments," Proceedings of the Symposium on Surface Water Impoundments, American Society of Civil Engineers, H. G. Stefan, ed., Vol II, Paper 7-20, pp 1404-1410.
- Contractor, D. N., and Wiggert, J. M. 1972. "Numerical Studies of Unsteady Flow in the James River," Bulletin 51, VPI-WRRC 51, Water Resources Research Center, Virginia Polytechnic Institute and State University, Blacksburg, Va.
- Dake, J. M. K., and Harleman, D. R. F. 1966. "An Analytical and Experimental Investigation of Thermal Stratification in Lakes and Ponds," Technical Report No. 99, Massachusetts Institute of Technology, Hydrodynamics Laboratory, Cambridge, Mass.
- Dortch, M. S. 1981 (Sep). "Investigation of Release Temperatures for Kinzua Dam, Allegheny River, Pennsylvania," Technical Report HL-81-9, US Army Engineer Waterways Experiment Station, Vicksburg, Miss.

- Dortch, M. S., et al. 1976 (Dec). "Dickey-Lincoln School Lakes Hydrothermal Study," Technical Report H-76-22, US Army Engineer Waterways Experiment Station, Vicksburg, Miss.
- Dronkers, J. J. 1969. "Tidal Computations for Rivers, Coastal Areas, and Seas," Journal, Hydraulics Division, American Society of Civil Engineers, Vol 95, No. HY1, pp 29-77.
- Edinger, J. E., and Geyer, J. C. 1965 (Jun). "Heat Exchange in the Environment," Publication No. 65-902, Edison Electric Institute, New York.
- Edinger, J. E., Duttweiler, D. W., and Geyer, J. C. 1968. "The Response of Water Temperatures to Meteorological Conditions," Water Resources Research, Vol 4, No. 5, pp 1137-1143.
- Edinger, J. E., Brady, D. K., and Geyer, J. C. 1974. "Heat Exchange and Transport in the Environment," EPRI Publication No. 74-049-00-3, Electric Power Research Institute, Palo Alto, Calif.
- Elder, R. A., and Wunderlich, W. 1968. "Evaluation of Fontana Reservoir Field Measurements," Proceedings of the Specialty Conference on Current Research into the Effects of Reservoirs on Water Quality, Vanderbilt University, Technical Report No. 17, p 221.
- Elder, S. W. 1959 (May). "The Dispersion of Marked Fluid in Turbulent Flow," Journal of Fluid Mechanics, Vol 5, Part 4, pp 544-560.
- Ellis, J. 1970. "Unsteady Flow in Channel of Variable Cross Section," Journal, Hydraulics Division, American Society of Civil Engineers, Vol 96, No. HY10, pp 1927-1945.
- Fontane, D. G., and Bohan, J. P. 1974. "Richard B. Russell Lake Water Quality Investigation; Hydraulic Model Investigation," Technical Report H-74-14, US Army Engineer Waterways Experiment Station, Vicksburg, Miss.
- Fontane, D. G., et al. 1977 (Apr). "Marysville Lake Hydrothermal Study; 900-MW Project; Hydraulic and Mathematical Model Investigation," Technical Report H-77-5, Report 1, US Army Engineer Waterways Experiment Station, Vicksburg, Miss.
- Ford, D. E. 1976. "Water Temperature Dynamics of Dimictic Lakes; Analysis and Predictions Using Integral Energy Concepts; Vols I and II," Ph. D. Dissertation, University of Minnesota, Minneapolis, Minn.
- Fread, D. L. 1971. Discussion of "Implicit Flood Routing in Natural Channels," by M. Amein and C. S. Fang, Journal, Hydraulics Division, American Society of Civil Engineers, Vol 97, No. HY7, pp 1156-1159.
- \_\_\_\_\_. 1973. "Technique for Implicit Dynamic Routing in Rivers with Tributaries," Water Resources Research, Vol 9, No. 4, pp 918-926.
- \_\_\_\_\_. 1978. "NWS Operational Dynamic Wave Model," Verification of Mathematical and Physical Models, Proceedings of 26th Annual Hydraulics Division Specialty Conference, American Society of Civil Engineers, College Park, Maryland, pp 455-464.

- Fread, D. L. 1980. "Capabilities of NWS Model to Forecast Flash Floods Caused by Dam Failures," Proceedings of the 2nd Conference on Flash Floods, American Meteorological Society, Atlanta, pp 171-178.
- \_\_\_\_\_. 1983. "Channel Routing; Lecture Notes for Unsteady Flow in Open Channels," February 28-March 9, Pennsylvania State University.
- Garrison, J. M., Granju, J. P., and Price, J. T. 1969. "Unsteady Flow Simulation in Rivers and Reservoirs," Journal, Hydraulics Division, American Society of Civil Engineers, Vol 95, No. HY5, pp 1559-1576.
- Goodrich, R. D. 1931. "Rapid Calculation of Reservoir Discharge," Civil Engineering, Vol 1, pp 417-418.
- Henderson, F. M. 1966. Open Channel Flow, Macmillan, New York, pp 356-362.
- Holland, J. P., and Dortch, M. S. 1982 (Apr). "Norfork Lake, Arkansas, Temperature Analysis; Mathematical Model Investigation," Technical Report HL-82-12, US Army Engineer Waterways Experiment Station, Vicksburg, Miss.
- Huber, W. C., and Harleman, D. R. F. 1968. "Laboratory and Analytical Studies of Thermal Stratification of Reservoirs," Technical Report No. 112, Ralph M. Parsons Laboratory for Water Resources and Hydrodynamics, Massachusetts Institute of Technology, Cambridge, Mass.
- Hutchinson, G. E. 1957. Treatise on Limnology; Vol I: Geography, Physics, and Chemistry, Wiley, New York.
- Isaacson, E., Stoker, J. J., and Troesch, A. 1956. "Numerical Solution of Flood Prediction and River Regulation Problems; Report III," IMM-NYU-235, New York University, Institute of Mathematical Science, New York.
- Jirka, G. A., and Harleman, D. R. F. 1979. "Cooling Impoundments: Classification and Analysis," Journal, Energy Division, American Society of Civil Engineers, Vol 105, No. EY2, pp 291-309.
- Jirka, G. A. and Watanabe, M. 1980 (May). "Thermal Structure of Cooling Ponds," Journal, Hydraulics Division, American Society of Civil Engineers, No. HY5, pp 701-715.
- Johnson, B. H. 1974 (Sep). "Unsteady Flow Computations on the Ohio-Cumberland-Tennessee-Mississippi River System," Technical Report H-74-8, US Army Engineer Waterways Experiment Station, Vicksburg, Miss.
- Kittrell, F. W. 1965. "Thermal Stratification in Reservoirs," Symposium on Streamflow Regulation for Quality Control, US Department of Health, Education, and Welfare, p 57.
- Knight, W. E. 1965. "Improvement of the Quality of Reservoir Discharges Through Control of Discharge Elevation," Symposium Streamflow Regulation for Quality Control, US Department of Health, Education, and Welfare, p 279.

- Lai, C. 1967. "Computation of Transient Flows in Rivers and Estuaries by the Multiple Reach Method of Characteristics," US Geological Survey Professional Paper 575-D, pp D273-D280.
- Liggett, J. A., and Woolhiser, D. A. 1967. "Difference Solutions of the Shallow-Water Equation," Journal, Engineering Mechanics Division, American Society of Civil Engineers, Vol 95, No. EM2, pp 39-71.
- Martin, C. S., and DeFazio, F. G. 1969. "Open Channel Surge Simulation by Digital Computer," Journal, Hydraulics Division, American Society of Civil Engineers, Vol 95, No. HY6, pp 2049-2070.
- Oliver, J. L., Hudson, P. L., and Clayton, J. P. 1977. "Effects of Pumped Storage Hydroelectric Plant on Reservoir Trout Habitat," Southeast Reservoir Investigations, US Fish and Wildlife Service, Clemson, S. C.
- Orlob, G. T. 1969 (Dec). "Mathematical Models for Prediction of Thermal Energy Changes in Impoundments," Final Report for Reservoir Water Quality Association by Water Resources Engineers, Inc., Walnut Creek, Calif.
- Potter, D. U., Stevens, M. P., and Meyer, J. L. 1982. "Changes in Physical and Chemical Variables in a New Reservoir Due to Pumped Storage Operations," Water Resources Bulletin, American Water Resources Association, Vol 18, No. 4, pp 627-633.
- Preissmann, A. 1961. "Propagation of Translatory Waves in Channels and Rivers," Proceedings, First Congress of French Association for Computation, Grenoble, France, pp 433-442.
- Puls, L. G. 1928. "Construction of Flood Routing Curves," House Document 185, US 70<sup>th</sup> Congress, 1<sup>st</sup> Session, Washington, DC, pp 46-52.
- Roberts, P. J. W. 1981 (Mar). "Jet Entrainment in Pumped-Storage Reservoirs," Technical Report E-81-3, US Army Engineer Waterways Experiment Station, Vicksburg, Miss.; under contract by Georgia Institute of Technology.
- Saint-Venant, B. de. 1871. "Theory of the Nonpermanent Movement of Waters with Application to the Floods of Rivers and to the Introduction of the Tides Within Their Beds," Comptes rendus, Vol 73, pp 147-154, 237-240, Academy of Science, Paris; Translated into English by the US Army Waterways Experiment Station, Vicksburg, Miss., and published as Translation No. 49-9, 1949.
- Simmons, G. M. 1976. "The Smith Mountain-Leesville Project: A Case History," Transactions of the American Fish Society, Vol 105, pp 173-180.
- Stoker, J. J. 1953. "Numerical Solution of Flood Prediction and River Regulation Problems; Report I, Deviation of Basic Theory and Formulation of Numerical Methods of Attack," Report No. IMM-NYU-200, New York University, Institute of Mathematical Science, New York.

Streeter, V. L., and Wylie, E. B. 1967. Hydraulic Transients, McGraw, New York, pp 239-259.

Strelkoff, T. 1969 (May). "The One-Dimensional Equations of Open-Channel Flow," Journal, Hydraulics Division, American Society of Civil Engineers, Vol 95, No. HY3, pp 861-874.

Wylie, E. B. 1970. "Unsteady Flow in Channel of Variable Cross Section," Journal, Hydraulics Division, American Society of Civil Engineers, Vol 96, No. HY11, pp 2241-2251.

Zimmerman, M. J. and Dortch, M. S. 1986 (Feb). "Water Quality Model Study of Proposed Reregulation Dam Downstream from Buford Dam, Chattahoochee River, Georgia" (in preparation), US Army Engineer Waterways Experiment Station, Vicksburg, Miss.

Table 1  
Corps of Engineers Reregulation Pool Systems

Reregulation Pool	Upper Reservoir	Remarks
Carters Reregulation Pool Maximum storage 17.5 KAF Surface area at maximum storage of 0.87 KA Length 1.5 miles	Carters Reservoir Maximum storage 473 KAF Surface area at maximum storage 3.22 KA	Coosawatter River, Georgia Average flow 770 cfs Hydropower pumped-storage system
DeGray Reregulation Pool Maximum storage 3 KAF Surface area at maximum storage 0.43 KA Length 2 miles	DeGray Lake Maximum storage 655 KAF Surface area at maximum storage 17 KA	Caddo River, Arkansas Average flow 726 cfs Hydropower pumped-storage system
Clarence Cannon Reregulation Pool Maximum storage 8.4 KAF Surface area at maximum storage 1.02 KA Length 9.5 miles	Mark Twain Lake Maximum storage 2,060 KAF Surface area at maximum storage 38.4 KA	Salt River, Missouri Average flow 1,530 cfs Hydropower pumped-storage system
B. A. Steinhagen Lake Storage at interim level 94.2 KAF Surface area at interim level 13.7 KA Length 30 miles	Sam Rayburn Dam and Reservoir Maximum storage 4,000 KAF Surface area at maximum storage 143 KA	Angelina River, Texas Average flow 2,800 cfs Maintains flow to reduce salinity intrusion
Broken Bow Reregulation Pool Design pool storage 9.5 KAF Design pool surface area 0.53 KA Length 3 miles	Broken Bow Reservoir Maximum storage 1,370 KAF Surface area at maximum storage 18 KA	Mountain Fork River, Oklahoma Average flow 1,300 cfs Hydropower reregulation and to satisfy low flow requirements
Keystone Reregulation Pool Maximum storage 3.5 KAF Length 8 miles	Keystone Lake Maximum storage 1,840 KAF Surface area at maximum storage 55.3 KA	Arkansas River, Oklahoma Average flow 6,400 cfs Built to maintain minimum flows for water quality at Tulsa and to moderate hydropower releases
Bonneville Lake Normal maximum storage 537 KAF at normal maximum surface area 20.4 KA Length 4.5 miles	The Dalles Maximum storage at 200,000 cfs 859 KAF	Columbia River, Washington and Oregon Average flow 194,300 cfs Reregulation to meet tailwater restrictions
Foster Reservoir Maximum storage 61 KAF Surface area at maximum storage 1.22 KA	Green Peter Reservoir Maximum storage 430 KAF Surface area at maximum storage 3.72 KA	South Santiam River, Oregon Average flow 1,530 cfs Provides flood control and hydro-power reregulation
Big Cliff Reregulation Pool Total storage 6.45 KAF Surface area at maximum pool 0.141 KA Length 2.8 miles	Detroit Reservoir Maximum storage 455 KAF	North Santiam River, Oregon Average flow 1,940 cfs Hydropower reregulation
Dexter Reregulation Pool Total storage 27.5 KAF Surface area at normal pool 1.03 KA Length 2.7 miles	Lookout Point Reservoir Normal storage 420 KAF Normal surface area 4.2 KA	Middle Fork Willamette River, Oregon Average flow 2,525 cfs Hydropower reregulation and hydro-power production

NOTE: The Dardanelle Reservoir, Arkansas, was also mentioned as having reregulation capability; however it is rarely used in that capacity. KA = Kiloacre, KAF = Kiloacre-feet, cfs = cubic feet per second.

Table 2  
Temperature Fluctuation for a Hypothetical  
Reregulation Pool Site

<u>Cycle Period, days</u>	<u>Temperature Amplitude</u> (Water Temperature Amplitude/Equilibrium Temperature Amplitude)	
	<u>Reregulation Pool</u>	<u>Natural Conditions</u>
1	0.04	0.02
365	0.81	0.53
$\infty$	0.82	0.53

Simulation Conditions

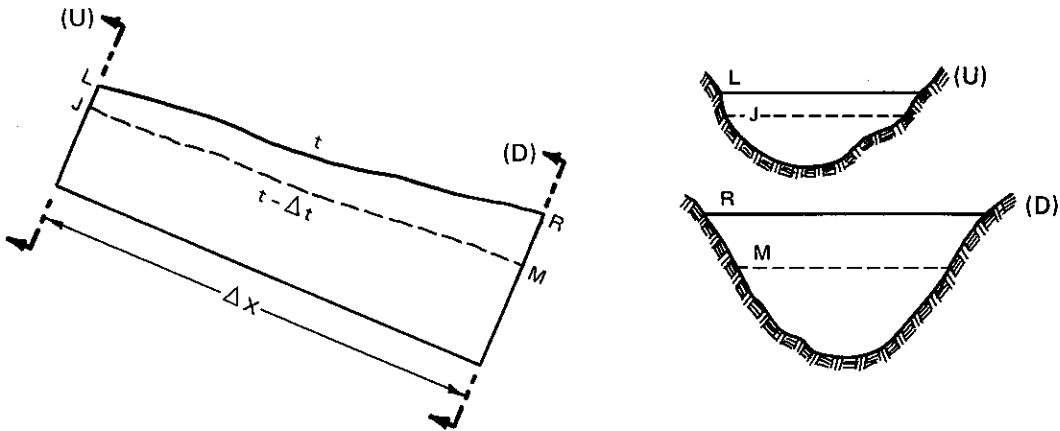
Volume, KAF*	10.0	5.0
Surface Area, KA**	1.0	0.25
Flow Rate, KAF/D†	0.5	0.5

---

\* KAF = Kiloacre-feet.  
 \*\* KA = Kiloacre.  
 † KAF/D = Kiloacre-feet/day.

## APPENDIX A: SAINT-VENANT EQUATIONS

1. The Saint-Venant equations, in the form used in this study, may be derived as follows:



The elementary water cell is a portion of the stream with cell walls perpendicular to the trace of the channel bottom. The downstream is designated as section (D) and the upstream as (U). The water positions M and R designate the instantaneous water position at section (D) at times  $t - \Delta t$  and  $t$ , respectively. Likewise, J and L indicate the instantaneous water position for section (U).

2. The conservation of mass of an incompressible fluid, described as the increase in volume of the segment over a time period  $\Delta t$ , would simply be the volume passing into the segment subtracting the flow leaving.

If

$$\bar{Q}_u = \text{time-averaged inflow across section (U)}$$

$$\bar{Q}_D = \text{time-averaged flow out of the segment through the downstream segment}$$

then volume increase would be

$$V(t) - V(t-\Delta t) = (\bar{Q}_u - \bar{Q}_D) \Delta t$$

If  $\bar{\sim}$  is used to denote the average instantaneous value of a given

parameter over length  $\Delta x$  (i.e.,  $\tilde{A}$  represents the average instantaneous cross-sectional area over length  $\Delta x$ ), then

$$\tilde{A}(t)\Delta x - \tilde{A}(t - \Delta t)\Delta x = (\bar{Q}_u - \bar{Q}_D)\Delta t \quad (A1)$$

The sign convention is chosen for  $x$  positive to the right. Dividing by  $\Delta x\Delta t$  yields

$$\frac{\tilde{A}(t) - \tilde{A}(t - \Delta t)}{\Delta t} = \frac{\bar{Q}_u - \bar{Q}_D}{\Delta x} \quad (A2)$$

Noting that  $Q_D - Q_U$  is the same as  $\bar{Q}(x + \Delta x) - \bar{Q}(x)$  and assuming  $A$  and  $Q$  are sufficiently smooth over the region  $\Delta x$ , and  $\Delta x$  and  $\Delta t$  approach 0. Then

$$\frac{\partial A}{\partial t} + \frac{\partial Q}{\partial x} = 0 \quad (A3)$$

This is the continuity equation.

3. Conservation of momentum means that the net rate of momentum entering an element plus the sum of the forces acting on the element equals the rate of accumulation of momentum.

4. Representing the net rate of momentum entering an element on the upstream face is

$$\rho \left( \frac{Q_u^2}{Au} \right)$$

if a uniform velocity distribution is assumed then,

$$u = V \frac{Q}{A}$$

so the momentum flux through a section is

$$Q(\rho u) = Q\left(\rho \frac{Q}{A}\right) = \rho \left(\frac{Q^2}{A}\right)$$

5. Representing the new rate of momentum entering an element on the downstream face is

$$-\rho \left(\frac{Q_D^2}{A_D}\right)$$

6. The forces acting on an element are listed below.

a. Pressure forces:

$$P_{UDT} = P_U - P_D + P_T$$

where

$P_U$  = pressure force on the upstream face

$P_D$  = pressure force on the downstream face

$P_T$  = x component pressure forces on the sidewalls of the element

b. Weight force:

$$W = g S_o \tilde{A} \Delta x \quad (A4)$$

This is a component of weight force directed along the x axis. So is the bottom slope equal to sin of the angle between the x direction and the horizontal.

c. Friction force:

$$D = -\rho g \tilde{S}_f A \Delta x \quad (A5)$$

7. The momentum within an element can be expressed as

$$M(t) = \rho \tilde{Q}(t) \Delta x \quad (A6)$$

8. Therefore, the discrete conservation statement would be

$$\Delta t \left[ \rho \left( \frac{\bar{Q}_u^2}{A_u} - \frac{\bar{Q}_D^2}{A_D} \right) + \rho g \tilde{S}_o \tilde{A} \Delta x - \rho g \tilde{S}_f \tilde{A} \Delta x + P_U - P_D + P_T \right] = \rho \tilde{Q}(t) \Delta x - \rho \tilde{Q}(t - \Delta t) \Delta x \quad (A7)$$

If the flow depths  $y$  and widths  $B$  change gradually over the length of the cell, then the derivatives  $\partial B/\partial x$  and  $\partial Y/\partial x$  exist. Further, if the pressure distribution is assumed hydrostatic and that the bottom slope is small, then the pressure force on a face is given by:

$$P = \rho g \int_0^Y (Y - \eta) B(x, \eta) d\eta \quad (A8)$$

where  $\eta$  is 0 at the channel bottom and  $Y$  at the surface

$$P_T = \rho g \Delta x \int_0^{\tilde{Y}} (\tilde{Y} - \eta) \frac{\partial \tilde{B}}{\partial x} d\eta \quad (A9)$$

So,

$$P_U - P_D + P_T = P_T - \frac{\partial P}{\partial x} \Delta x \quad (A10)$$

$$\frac{\partial P}{\partial x} \Delta x = \rho g \Delta x \frac{\partial}{\partial x} \int_0^{\tilde{Y}} (\tilde{Y} - \eta) \tilde{B} d\eta \quad (A11)$$

from Liebnitz's Rule

$$\rho g \Delta x \frac{\partial}{\partial x} \int_0^{\tilde{Y}} (\tilde{Y} - \eta) \tilde{B} d\eta = \rho g \Delta x \left[ \int_0^{\tilde{Y}} \frac{\partial (\tilde{Y} - \eta) (B) d\eta}{\partial x} + (\tilde{Y} - \tilde{Y}) B(y) \frac{\partial \tilde{Y}}{\partial x} - (\tilde{Y} - 0) \tilde{B}(0) \frac{\partial 0}{\partial x} \right] \quad (A12)$$

$$\frac{\partial P}{\partial x} \Delta x = \rho g \Delta x \left[ \int_0^{\tilde{Y}} \frac{\partial \tilde{Y}}{\partial x} \tilde{B} d\eta + \int_0^{\tilde{Y}} (\tilde{Y} - \eta) \frac{\partial \tilde{B}}{\partial x} d\eta \right] \quad (A13)$$

$$P_T - \frac{\partial P}{\partial x} \Delta x = \rho g \Delta x \left[ \int_0^{\tilde{Y}} (\tilde{Y} - \eta) \frac{\partial \tilde{B}}{\partial x} d\eta - \int_0^{\tilde{Y}} \frac{\partial \tilde{Y}}{\partial x} \tilde{B} d\eta - \int_0^{\tilde{Y}} (\tilde{Y} - \eta) \frac{\partial \tilde{B}}{\partial x} d\eta \right] \quad (A14)$$

$$P_T - \frac{\partial P}{\partial x} \Delta x = \rho g \Delta x \left[ \int_0^{\tilde{Y}} (\tilde{Y} - \eta) \frac{\partial \tilde{B}}{\partial x} d\eta - \int_0^{\tilde{Y}} \frac{\partial \tilde{Y}}{\partial x} \tilde{B} d\eta - \int_0^{\tilde{Y}} (\tilde{Y} - \eta) \frac{\partial \tilde{B}}{\partial x} d\eta \right] \quad (A15)$$

$$P_U - P_D + P_T = P_T - \frac{\partial P}{\partial x} \Delta x = -\rho g \Delta x \int_0^{\tilde{Y}} \frac{\partial \tilde{Y}}{\partial x} \tilde{B} d\eta = -\rho g \Delta x \tilde{A} \frac{\partial \tilde{Y}}{\partial x} \quad (A16)$$

9. If the weight force is included with the pressure force

$$P_U - P_D + P_T + W = -\rho g \Delta x \tilde{A} \frac{\partial \tilde{h}}{\partial x} \quad (A17)$$

where  $h$  is the water-surface elevation.

10. Dividing the discrete momentum equation by  $\rho g \Delta x \Delta t$  leaves

$$\frac{1}{g} \left( \frac{\tilde{Q}_U^2}{A_U} - \frac{\tilde{Q}_D^2}{A_D} \right) / \Delta x + \tilde{A} \tilde{S}_o - \tilde{A} \tilde{S}_f + (P_U - P_D + P_T) / \rho g \Delta x = \frac{1}{g} \frac{\tilde{Q}(y) - \tilde{Q}(t - \Delta t)}{\Delta t} \quad (A18)$$

As  $\Delta x$  and  $\Delta t \rightarrow 0$ , and substituting the weight and pressure force derivation and rearranging leaves:

$$\frac{\partial Q}{\partial t} + \frac{\partial(Q^2/A)}{\partial x} + gA \left( \frac{\partial h}{\partial x} + S_f \right) = 0 \quad (A19)$$

APPENDIX B: HYDRODYNAMIC CODE

1. The development of the finite difference formulation uses a four-point method. The time indicator is given in the following equations by a superscript "N", where N represents the n<sup>th</sup> time step. Similarly, distance is given by the subscript "i". The spatial derivatives for a segment employed a time weighting factor  $\theta$  which may vary from 0.5 to 1. A value of 0.5 provides equal weighting of the values at the N and N + 1 time steps. Thus, the finite difference formulation for continuity used is:

$$\theta(Q_{i+1}^{N+1} - Q_i^{N+1}) + (1 - \theta)(Q_{i+1}^N - Q_i^N) + 0.5 \frac{\Delta x}{\Delta t} (A_i^{N+1} + A_{i+1}^{N+1} - A_i^N - A_{i+1}^N) = 0 \quad (B1)$$

and the momentum equation representation is:

$$0.5 \frac{\Delta x}{\Delta t} (Q_{i+1}^{N+1} + Q_i^{N+1} - Q_i^N - Q_{i+1}^N) + \theta \left[ \left( \frac{Q^2}{A} \right)_{i+1}^{N+1} - \left( \frac{Q^2}{A} \right)_i^{N+1} + g \bar{A}_i^{N+1} (h_{i+1}^{N+1} - h_i^{N+1} + \Delta x \bar{S}_{f_i}^{N+1}) \right] + (1 - \theta) \left[ \left( \frac{Q^2}{A} \right)_{i+1}^N - \left( \frac{Q^2}{A} \right)_i^N + g \bar{A}_i^N (h_{i+1}^N - h_i^N + \Delta x \bar{S}_{f_i}^N) \right] = 0 \quad (B2)$$

where

$$\bar{A}_i = 0.5 (A_{i+1} + A_i)$$

$$\bar{S}_{f_i} = \frac{\bar{n}_i^2 \bar{Q}_i \bar{Q}_i}{2.21 \bar{A}_i^2 R^{4/3}}$$

$B_i$  = top width of segment  $i$

$$\bar{Q}_i = 0.5 (Q_{i+1} + Q_i)$$

Notice that the values of  $Q$ ,  $A$ , and  $h$  are known at the  $N^{\text{th}}$  time steps so the equations may be rewritten with the unknowns on the left-hand side as

$$0.5 \frac{\Delta x}{\Delta t} A_i^{N+1} - \theta Q_i^{N+1} + 0.5 \frac{\Delta x}{\Delta t} A_{i+1}^{N+1} + \theta Q_{i+1}^{N+1} = \text{RHS} \quad (\text{B3})$$

and

$$\begin{aligned} -g \theta \bar{A}_i^{N+1} h_i^{N+1} + 0.5 \frac{\Delta x}{\Delta t} Q_i^{N+1} + g \theta \bar{A}_i^{N+1} h_{i+1}^{N+1} + 0.5 \frac{\Delta x}{\Delta t} Q_{i+1}^{N+1} \\ + \theta \left( \frac{Q^2}{A} \right)_{i+1}^{N+1} - \theta \left( \frac{Q^2}{A} \right)_i^{N+1} + g \theta \bar{A}_i^{N+1} \Delta x \bar{S}_f^{N+1} = \text{RHS} \end{aligned} \quad (\text{B4})$$

Equation B4, however, contains nonlinear terms so the solution cannot be found directly. The solution proceeds by an iterative solution using the nonlinear Newton-Raphson iteration technique.

2. In the Newton-Raphson technique the residuals of Equations B1 and B2 are evaluated from a prior estimate and the solution is found by iterative corrections to the previous estimate. If Equation B1 is designated by  $C$  and Equation B2 by  $M$ , then corrections to  $h_i^{N+1}$ ,  $h_{i+1}^{N+1}$ ,  $Q_i^{N+1}$ , and  $Q_{i+1}^{N+1}$ , may be found by

$$\frac{\partial C}{\partial h_i} \Delta h_i + \frac{\partial C}{\partial Q_i} \Delta Q_i + \frac{\partial C}{\partial h_{i+1}} \Delta h_{i+1} + \frac{\partial C}{\partial Q_{i+1}} \Delta Q_{i+1} = -C \quad (\text{B5})$$

$$\frac{\partial M}{\partial h_i} \Delta h_i + \frac{\partial M}{\partial Q_i} \Delta Q_i + \frac{\partial M}{\partial h_{i+1}} \Delta h_{i+1} + \frac{\partial M}{\partial Q_{i+1}} \Delta Q_{i+1} = -M \quad (\text{B6})$$

These calculations are made for each segment over the length of the simulated reach in combination with the boundary conditions from which the values of  $\Delta h_i$ ,  $\Delta h_{i+1}$ ,  $\Delta Q_i$ , and  $\Delta Q_{i+1}$  may be found by solving the system of equations resulting from Equations B5 and B6. The superscript N+1 is understood throughout if no superscript is given. The various partial derivatives are evaluated as follows:

$$\frac{\partial C}{\partial h_i} = 0.5 \frac{\Delta x}{\Delta t} \frac{\partial A_i}{\partial h_i} = 0.5 \frac{\Delta x}{\Delta t} \left( B_i + \frac{\partial B_i}{\partial h_i} h_i \right) \quad (B7)$$

$$\frac{\partial C}{\partial Q_i} = \theta \frac{\partial(-Q_i)}{\partial Q_i} = -\theta \quad (B8)$$

$$\frac{\partial C}{\partial h_{i+1}} = 0.5 \frac{\Delta x}{\Delta t} \frac{\partial A_{i+1}}{\partial h_{i+1}} = 0.5 \frac{\Delta x}{\Delta t} \left( B_{i+1} + \frac{\partial B_{i+1}}{\partial h_{i+1}} h_{i+1} \right) \quad (B9a)$$

$$\frac{\partial C}{\partial Q_{i+1}} = \theta \frac{\partial Q_{i+1}}{\partial Q_{i+1}} = \theta \quad (B9b)$$

$$\frac{\partial M}{\partial h_i} = \theta \left[ \left( \frac{Q^2}{A^2} \right)_i \left( B_i + \frac{\partial B_{i+1}}{\partial h_{i+1}} h_i \right) + \frac{g}{2} \left( B_i + \frac{\partial B_i}{\partial h_i} h_i \right) (h_{i+1} - h_i \Delta x \bar{S}_{f_i}) + \bar{g} A_i \left( -1 + \Delta x \frac{\partial \bar{S}_{f_i}}{\partial h_i} \right) \right] \quad (B10)$$

$$\frac{\partial M}{\partial Q_i} = 0.5 \frac{\Delta x}{\Delta t} + \theta \left[ -2 \left( \frac{Q}{A} \right)_i + \bar{g} A_i \Delta x \frac{\partial \bar{S}_{f_i}}{\partial Q} \right] \quad (B11)$$

$$\frac{\partial M}{\partial h_{i+1}} = \theta \left[ \left( -\frac{Q^2}{A^2} \right)_{i+1} \left( B_{i+1} + \frac{\partial B_{i+1}}{\partial h_{i+1}} h_{i+1} \right) + \frac{g}{2} \left( B_{i+1} + \frac{\partial B_{i+1}}{\partial h_{i+1}} h_{i+1} \right) \right. \\ \left. \times \left( h_{i+1} - h_i + \Delta x \bar{S}_{f_i} \right) + g \bar{A}_i \left( 1 + \Delta x \bar{S}_{f_i} \right) \right] \quad (B12)$$

$$\frac{\partial M}{\partial Q_{i+1}} = 0.5 \frac{\Delta x}{\Delta t} + \theta \left[ 2 \left( \frac{Q}{A} \right)_{i+1} + g \bar{A}_i \Delta x \frac{\partial \bar{S}_{f_i}}{\partial Q} \right] \quad (B13)$$

The new estimates for  $h_i^{N+1}$ ,  $h_{i+1}^{N+1}$ ,  $Q_i^{N+1}$ , or  $Q_{i+1}^{N+1}$  were found by

$$f_i \text{ (new)} = f_i \text{ (old)} + \Delta f \quad (B14)$$

where  $f$  is any one of  $h_i^{N+1}$ ,  $h_{i+1}^{N+1}$ ,  $Q_i^{N+1}$ , or  $Q_{i+1}^{N+1}$  values. If  $\Delta f$  is sufficiently small, the  $f$  values are specified as solutions. If convergence has not been reached, these new estimates are used to generate updated estimates with the procedure just described.

3. The terms involving  $\frac{\partial B}{\partial h} h$  in this method were originally neglected; however, it was quickly discovered that changes in depth and width in a reregulation pool occur much too rapidly to drop these terms.

4. To close the system of equations, conditions on external boundaries must be specified. In this case, a discharge history  $Q(t)$  was designated both upstream and downstream. This condition can be handled as demonstrated by Fread (1983)\* with the boundary equation

$$G = Q_i^{N+1} - Q(t) = 0 \quad (B15)$$

---

\* References cited in the appendixes are included in the references at the end of the main text.

where

$$\frac{\partial G}{\partial Q_1} = 1$$

$$\frac{\partial G}{\partial h_1} = 0$$

for the upstream boundary ( $i = 1$ ) and

$$\frac{\partial G}{\partial Q_L} = 1$$

$$\frac{\partial G}{\partial h_L} = 0$$

for the downstream boundary ( $i = L$ ).

5. The coefficient matrix is banded with most of the elements being zero except for four elements in each row adjacent to the main diagonal. An efficient solution technique developed by Fread (1971), in which the computations do not involve zero elements is used. This reduces the number of matrix operations from  $(16/3N^3 + 8N^2 + 14/3N)$  to  $(38N - 19)$  where  $N$  is the total number of cross sections along the pool; further, the code stores only the nonzero elements and so reduces storage for the required coefficients matrix from  $2N \times 2N$  to  $2N \times 4$ .

APPENDIX C: TRANSPORT CODE

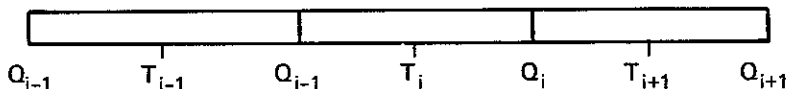
1. The partial differential equation approximated by this code for temperature is

$$\frac{\partial(AT)}{\partial t} + \frac{\partial(QT)}{\partial x} - \frac{\partial}{\partial x} E_L \frac{\partial(AT)}{\partial x} = \frac{KB(T_E - T)}{\gamma c_p} \quad (C1)$$

where

- A = cross-sectional area
- T = temperature
- Q = discharge rate
- $E_L$  = longitudinal dispersion coefficient
- K = surface-heat exchange coefficient
- B = top width
- $T_E$  = equilibrium temperature
- $\gamma$  = weight density
- $c_p$  = specific heat

In the finite difference formulation, the spatial derivatives are replaced by centered differences in the dispersion term by Roache's first-order windward differencing scheme for the advective term. The windward scheme preserves the transportive property but is only of first order. The temporal derivative is also only of first order. So the overall scheme is approximately  $(\Delta t, \Delta x)$ . The scheme used is implicit so that the time step restriction  $\Delta V/Q$  is removed where  $\Delta V$  = incremental segment volume. The finite difference formulation therefore is:



$$\begin{aligned}
& \frac{(\bar{A}T_i)^{N+1} - (\bar{A}T_i)^N}{\Delta t} \\
& + \frac{\left\{ Q_i^{N+1} \left[ \psi T_i^{N+1} + (1 - \psi) T_{i+1}^{N+1} \right] - Q_{i-1}^{N+1} \left[ \phi T_{i-1}^{N+1} + (1 - \phi) T_i^{N+1} \right] \right\}}{\Delta x} \\
& - \frac{\left[ E_{Li} A_i^{N+1} (T_{i+1}^{N+1} - T_i^{N+1}) - E_{Li-1} A_{i-1}^{N+1} (T_i^{N+1} - T_{i-1}^{N+1}) \right]}{(\Delta x)^2} \\
& = \frac{K\bar{B}^{N+1} \left[ T_E(t) - T_i^{N+1} \right]}{\gamma_c^p} \quad (C2)
\end{aligned}$$

where  $\bar{A}_i = 0.5 (A_i + A_{i-1})$

and  $\bar{B}_i = 0.5 (B_i + B_{i-1})$

The superscript N indicates the specific time step and i indicates the longitudinal location as shown below.

2. All information such as Q, A, and V, which are supplied by the hydrodynamic model, are defined at the segment ends as shown in the figure for the Q parameter. The constituent concentration or temperature is defined at the center of the segment.

3. All information used in this formulation is known from the hydrodynamic model results and from previously calculated temperatures except for  $T_{i-1}^{N+1}$ ,  $T_i^{N+1}$ , and  $T_{i+1}^{N+1}$  for each segment i. The coefficients of these parameters are then grouped so that the resulting system of equations has the form:

$$C_1 T_{i-1}^{N+1} + C_2 T_i^{N+1} + C_3 T_{i+1}^{N+1} = C_4 \quad (C3)$$

where

$$C_1 = \frac{-\phi Q_{i-1}^{N+1}}{\Delta x} + \frac{E_{Li-1} A_{i-1}^{N+1}}{(\Delta x)^2}$$

$$C_2 = \frac{\bar{A}^{N+1}}{\Delta t} + \frac{\psi Q_i^{N+1} - (1 - \phi) Q_{i-1}^{N+1}}{\Delta x} + \frac{E_{Li-1} A_{i-1}^{N+1} + E_{Li} A_i^{N+1}}{(\Delta x)^2} + \frac{K\bar{B}^{N+1}}{\gamma c_p}$$

$$C_3 = \frac{(1 - \psi) Q_i^{N+1}}{\Delta x} - \frac{E_{Li} A_i^{N+1}}{(\Delta x)^2}$$

$$C_4 = \frac{\bar{A}^N T_i^N}{\Delta t} + \frac{K\bar{B}^{N+1}}{\gamma c_p}$$

where

$$\phi = 1 \text{ for } Q_{i-1} > 0$$

$$\phi = 0 \text{ for } Q_{i-1} \leq 0$$

$$\psi = 1 \text{ for } Q_i > 0$$

$$\psi = 0 \text{ for } Q_i \leq 0$$

$$\bar{A} = \frac{(A_{i-1} + A_i)}{2}$$

$$\bar{B} = \frac{(B_{i-1} + B_i)}{2}$$

The upstream boundary condition is defined as the temperature supplied from upstream by flow from the upper dam. The downstream boundary is allowed only to advect temperature, or whatever constituent is being

considered, out of the system. It does not disperse the constituent out as this is usually a solid (structural) boundary. This is also true at the upstream boundary during pumpback.

4. The resulting matrix is solved for temperature at each segment by a very efficient tridiagonal solver known as the Thomas algorithm. The concentration of a constituent can be computed in the same manner illustrated by this example for temperature with a modification of the source-sink term given on the right-hand side of Equation C1.

APPENDIX D: NOTATION

A	Cross-sectional area; horizontal area of the element, $\text{ft}^2$ ; cross-sectional area at a given longitudinal location
$A_n$	Surface area of reservoir
B	Width
$c_p$	Specific heat of water
C	Constituent concentration
D	Channel depth of flow
$D_v$	Vertical entrance dilution
e	Average normalized density gradient taken as $0.3 \times 10^{-6}/\text{ft}$
$E_L$	Longitudinal dispersion coefficient
$f_i$	Interfacial friction factor
$F_D$	Densimetric-Froude number
g	Gravitational acceleration constant
h	Water-surface elevation above datum; water-surface elevation
H	Average pond depth
$H_s$	Net rate of surface-heat
i	Cross-section number
I	Inflow
K	Coefficient of surface-heat exchange; vertical diffusion coefficient, $\text{ft}^2/\text{day}$
K and $T_E$	Surface-heat exchange component
KA	Kiloacre
KAF	Kiloacre-feet
KAF/D	Kiloacre-feet/D
L	Total pond length
n	1 or 2, denoting the main reservoir and reregulation pool, respectively; Manning's $n$
O	Outflow
P	Pond number

$P_D$	Pressure force on the downstream face
$P_T$	X component pressure forces on the sidewalls of the element
$P_U$	Pressure force on the upstream face
$Q$	Flow-through rate in cfs; flow through the reach; discharge
$Q_i$	Inflow rate, cfs/day; upstream discharge of segment i
$Q_{in}$	Input to reregulation pool (generation)
$Q_o$	Condenser flow rate; withdrawal rate, cfs/day
$Q_{out}$	Outflow from the reregulation pool (pumpback and/or downstream release)
$Q_v$	Net vertical flow into or out of a layer
$Q_1$	Inflow and outflow rate; flow rate in generation (from reservoir 1 to 2)
$Q_2$	Pumpback rate (flow rate from 2 to 1)
$Q_3$	Net flow rate through entire system (equal to the inflow to reservoir, and also the release from reservoir 2)
$R$	Ratio of yearly reservoir inflow volume to actual reservoir volume for a number of impoundments in the continental United States; hydraulic radius
$R < R_c$	Criterion for presence of reservoir stratification
$S$	Storage; sources and sinks for the given constituent
$S_f$	Friction slope
$S_l$	Source or sink
$t$	Time
$T$	Water-surface temperature; temperature
$T_c$	Cycle period
$T_i$	Intake temperature (from pond); temperature of the inflow, °F
$T_n$	Temperature of reservoir
$T_o$	Discharge temperature (into pond); temperature of the withdrawal, °F
$T_E$	Equilibrium temperature
$T_I$	Inflow temperature
$T_i$	Instantaneous temperature of the reservoir and also the outflow temperature

$T_{1i}$	Initial temperature of reservoir 1
$T_{1ss}$	Ultimate steady-state temperature for main reservoir
$T_{2i}$	Initial temperature of reservoir 2
$T_{2ss}$	Ultimate steady-state temperature of reregulation pool
U	Constant, channel velocity
V	Volume of the reservoir in cubic feet; velocity; pool volume; volume of reach
$V_n$	Volume of reservoir n
$V_F$	Final volume
$V_I$	Initial volume
$V_1$	Volume of the reservoir
W	Average pond width
X	Weighting coefficient; distance along the waterway; longitudinal distance
$\alpha \sin \theta t$	Equilibrium temperature as a function of time
$\beta$	Coefficient of thermal expansion for water
$\gamma$	Specific weight of water
$\Delta S$	Change of storage within the reach during a time increment
$\Delta S_i$	Change in segment i storage
$\Delta t$	Time step length
$\Delta T_o$	Total temperature difference ( $T_o - T_i$ ) across pond
$\theta$	Cycle frequency = $2\pi/T_c$
$\rho$	Density of water, lb/ft <sup>3</sup>
x	Distance along longitudinal axis